TR- 114
1981

Texas Water Resources Institute
make every drop count

Contaminant Transport in Hydrogelogic Systems

C. Chin
D.L. Reddell

Texas Water Resources Institute

Texas A&M University

RESEARCH PROJECT COMPLETION REPORT

Project Number A-048-TEX

(October 1, 1978 - March 31, 1981)

Agreement Numbers

14-34-0001-9046
14-34-0001-0146
14-34-0001-1146

CONTAMINANT TRANSPORT IN HYDROGEOLOGIC SYSTEMS

Chia-Shyun Chen

Donald L. Reddell

The work on which this publication is based was supported in part by funds provided by the Office of Water Research and Technology (Project A-048-TEX), U. S. Department of the Interior, Washington, D.C., as authorized by the Water Research and Development Act of 1978.

Technical Report No. 114
Texas Water Resources Institute
Texas A&M University

March 1981

ABSTRACT

Contaminant Transport in Hydrogeologic Systems

by

Chia-Shyun Chen

and

Donald L. Reddell

Contaminant transport in hydrogeologic systems requires knowledge of transmissivity, storage coefficient, and dispersivity. Techniques for evaluating transmissivity and storage coefficient under field conditions are well known. However, the evaluation of dispersivity under field conditions is a costly and time consuming job.

The process of transporting a specific conservative ion species in an aquifer is analogous to the transport of heat in the system. Because of this analogy, the original objective of this research project was to evaluate the use of low-grade thermal water to measure aquifer dispersivity. However, available thermal models of groundwater aquifers proved difficult to use for evaluating the thermal properties (and dispersivity) of an aquifer. Therefore, additional objectives were developed to (1) derive analytical solutions describing the steady and unsteady temperature distribution around a well with a finite caprock thickness and (2) establish a technique for determining the thermal properties (including thermal dispersivity) of an aquifer using field measurements of temperature distribution within the aquifer.

Analytical models of hot water injection into groundwater aquifers were developed in this study. Available analytical models of this problem assume

that the caprock overlying the aquifer is of infinite thickness. However, many groundwater aquifers have caprock thicknesses of only a few meters. This paper shows two mathematical models which were developed to examine the influence of a caprock with finite thickness on the thermal response of an aquifer. In both models, the horizontal heat conduction and heat convection in the aquifer plus the vertical heat conduction in the caprock are considered. The first model (Model I) assumed that the vertical temperature gradient in the caprock is linear, which can be approached in a caprock with a relatively small thickness. The second model (Model II) removed this restriction and allowed the vertical temperature gradient in the caprock to be nonlinear. For Model I, a steady state and an unsteady state solution for the water temperature distribution surrounding an injection well were obtained. For Model II, a steady state and two unsteady state solutions for the water temperature distribution surrounding an injection well were obtained. One of the two unsteady state solutions is for a short-time period and the other one is for a long-time period.

A graphical technique was developed for determining four pertinent aquifer thermal properties: (1) the horizontal thermal conductivity of the aquifer (thermal dispersivity), (2) the thermal capacity of the aquifer, (3) the vertical thermal conductivity of the caprock, and (4) the thermal capacity of the caprock. Dimensionless type curves are constructed from the steady state solution and the unsteady state solution for short time periods in Model II, respectively. Using field data, one curve is constructed using long-term temperature observations (approaching steady state) from several observation wells, and a second curve is constructed using short-time temperature observations from any one of the observation wells. These curves are

ACKNOWLEDGEMENTS

The authors wish to express appreciation to Dr. John Nieber, Dr. David Norton, and Dr. Guy Curry for their review of the manuscript and their helpful comments and suggestions. Thanks are also expressed to Dr. Terry Howell and Dr. James Ruff for their helpful suggestions concerning this study.

A very special thank you is extended to Dr. Jay Walton of the mathematics department at Texas A&M University for his many helpful suggestions concerning the mathematical manipulations.

The authors are also grateful to the Department of Agricultural Engineering (Dr. E. A. Hiler, Head) and the Texas Water Resources Institute (Dr. J. R. Runkles, Director) for providing financial assistance for this study.

TABLE OF CONTENTS

		Page
ABSTRACT		iii
ACKNOWLEDGEMENTS		v
TABLE OF CONTENTS		vi
LIST OF TABLES		viii
LIST OF FIGURES		ix
Chapter		
I	INTRODUCTION	1
	Objective	3
	Scope	3
II	PREVIOUS WORK	5
	Thermal Response of Aquifers	5
	Evaluation of Aquifer Thermal Properties	9
	Summary	11
III	MATHEMATICAL REVIEW FOR THIS STUDY	13
	Transcendental Functions	13
	Laplace Transforms	20
	Laplace-Carson Transforms	22
IV	DEVELOPMENT OF MATHEMATICAL MODELS	25
	General Heat Equation in the Aquifer	27
	Partial Differential Equations for Model I.	29
	Partial Differential Equations for Model II	30

Chapter		Page
V	RESULTS AND DISCUSSIONS	33
	Analytical Solution for Model I	33
	Analytical Solutions for Model II	36
	Numerical Integration of Solutions	49
	Approximate Solution for Laplace Inversions	55
	Summary	56
VI	GRAPHICAL TECHNIQUES TO EVALUATE AQUIFER THERMAL PROPERTIES	59
	Illustration of the Graphical Technique	59
	Sample Calculations	62
	Discussion	68
	Approximate Graphical Method	71
VII	SUMMARY, CONCLUSIONS AND RECOMMENDATIONS	80
	Summary	80
	Conclusions	82
	Recommendations	83
REFERENCES		84
APPENDICES		87

LIST OF TABLES

Table		Page
1	Temperature measured at steady state condition	63
2	Temperautre measured at unsteady state condition (r = 40 m)	63

LIST OF FIGURES

Figure		Page
1	Schematic of aquifer heat transfer model	26
2	Type curves for short time period solution (η=0.5) . . .	42
3	Type curves for short time period solution (ω= 90) . . .	44
4	Type curves for steady state solution	47
5	Type curves for long time period solution (σ=10)	48
6	Type curves for long time period solution (ω=90)	50
7	Comparision of Schapery's approximate solution with exact solution	57
8	Curve matching steady state type curve with field data to evaluate values of K_m and K_r	64
9	Curve matching short time period type curve with field data to evaluate $(\rho C)_m$ and $(\rho C)_r$	67
10	Curve matching short time period type curve with field data to evaluate K_m and $(\rho C)_m$	74
11	Influence of $\pm$ 10 percent variation in K/α on short time period solution (ω=50)	76
12	Influence of $\pm$ 10 percent variation in K/α on short time period solution (ω=100)	77
13	Influence of $\pm$ 10 percent variation in K/α on short time period solution (ω=150)	78
14	Influence of $\pm$ 10 percent variation in K/α on short time period solution (ω=200)	79

CHAPTER I

INTRODUCTION

Thermal energy storage in aquifers is one of the most promising alternatives for seasonal storage of low-grade thermal energy. In the past, low-grade thermal energy has been stored in the form of hot or cold water in above-ground storage tanks. The size of such facilities are restricted by economic and space limitations. Thus, the storage of thermal water in above-ground water tanks is severely restricted. Since water can be injected, stored, and easily recovered from aquifers, the concept of aquifer thermal energy storage (ATES) has received much recent attention.

Davison et al. (1975) proposed that hot water produced by solar heaters during the summer be stored in aquifers and recovered during the winter for space heating. They also proposed that the winter's cold be used to chill water, which would then be stored in an aquifer and recovered during the summer for air conditioning. Davison et al. (1975) named their ATES system the "solaterre" system.

When injecting hot or cold fluids into confined aquifers, most of the thermal loss is caused by thermal conduction across the top and bottom of the aquifers. These losses decrease with time and approach a constant value. The effectiveness of ATES systems depends on the magnitude of the thermal losses from the system.

To evaluate these losses, temperature distributions around thermal injection wells are needed.

In this paper, results of analytical studies of thermal injection into confined aquifers are reported. These analytical studies provide an understanding of the basic principles involved when thermal energy is injected into an aquifer. In addition, analytical solutions:

1 Provide an understanding of the basic nature of the movement of the thermal front, and the relative importance of the variables involved in its propagation.

2 Provide a method for estimating the temperature distribution throughout an aquifer under a wide variety of conditions.

3 Provide assistance in interpreting results from laboratory tests, transposing these results to field experiments, and vice versa.

Most work in the area of thermal injection has been conducted in the field of petroleum engineering. Only recently has an interest in this area developed in the groundwater industry. Existing analytical models of this problem assume that the caprock overlying the aquifer is infinite in vertical extent. This condition can be approached in oil reservoirs. However, groundwater aquifers are found at depths of only a few meters. Obviously, assuming that the caprock is infinite in thickness can not be taken for granted in groundwater hydrology. Thus, it is important to investigate the influence of this assumption on the thermal response of aquifers.

The application of mathematical models to field problems of thermal injection requires the evaluation of thermal parameters involved in the partial differential equations. Usually, the thermal parameters

can not be measured directly, but must be determined from field measurements of temperature as a function of distance and time.

In recent years, considerable attention has been directed toward developing either graphical or numerical procedures for evaluating aquifer parameters. Numerical procedures to evaluate aquifer parameters have been developed which make extensive use of optimization principles and high speed computers. Graphical procedures, utilizing type curves constructed from analytical solutions and data plots prepared from field measurements, have also been used to evaluate aquifer properties. In the graphical method, field data plots are matched with the type curves and values of the aquifer parameters evaluated. A graphical method for evaluating aquifer thermal properties is developed in this study.

Objective

This study has the following objectives:

1 Develop an analytical solution describing the steady and unsteady temperature distribution around a well with a finite caprock thickness when hot water is injected.

2 Establish a technique for determining the thermal properties of an aquifer using field measurements of temperature distribution in the aquifer.

Scope

Two mathematical models are developed to examine the influence of the caprock thickness on the thermal response of an aquifer. The

first model assumes that the temperature distribution across a finite caprock thickness is linear; a condition which could be approached in a relatively thin caprock. The second model uses a caprock of finite thickness and allows the heat flux through the caprock to follow Fourier's Law. The graphical method for determining aquifer thermal properties employs the steady and unsteady state solutions from the second model.

Chapter II

PREVIOUS WORK

Thermal Response of Aquifers

Several analytical and numerical treatments of the problem of hot fluid injection into oil reservoirs or groundwater aquifers have been presented. For analytical models, some restrictive physical and mathematical assumptions must be made to obtain the analytical solutions. In numerical models, many of the restrictive assumptions used in the analytical models can be partially or totally removed. However, analytical solutions to mathematical models are still important in the study of many physical science and engineering problems. The scope of this paper is oriented toward an analytical study of the aquifer thermal injection problem.

Jenkins and Aronofsky (1954) studied three mechanisms of heat transfer during the injection of a hot fluid into an oil reservoir. The three mechanisms were:

1 Heat transfer due to the physical movement of the injected water.

2 Heat conduction from warmer to colder portions of the system.

3 Convective heat transfer between the sand grains in the reservoir and the surrounding fluid.

They indicated that convective transfer (mechanism 3) could be neglected by assuming that the temperature of the sand grains in the

reservoir and the surrounding fluid reached thermal equilibrium instantaneously. Since the work of Jenkins and Aronofsky (1954), mechanisms 1 and 2 have been widely adopted as the two most significant mechanisms of heat transfer in underground reservoirs.

Lauwerier (1955) presented an analytical solution for calculating the temperature distribution in a linear flow system. He neglected the horizontal heat conduction in the reservoir, and assumed that the vertical thermal conductivity in the reservoir was infinite so that no vertical temperature gradient existed across the reservoir. In the caprock, the horizontal thermal conductivity was assumed zero, but vertical heat conduction was considered.

Avdonin (1964) allowed horizontal heat conduction to occur in the reservoir, but kept the other assumptions in his model the same as those in Lauwerier's (1955) model. The analytical solution obtained by Avdonin was:

$$U = \frac{1}{\Gamma(\omega)} \left(\frac{r^2}{4\tau}\right)^{\omega} \int_0^1 \exp\left(\frac{-r^2}{4\tau x}\right) \cdot \operatorname{Erfc}\left(\frac{Kx\sqrt{\tau}}{2\alpha\sqrt{1-x}}\right) \frac{dx}{x^{1+\omega}}, \quad \ldots \quad [1]$$

where $U = \dfrac{T - T_o}{T_i - T_o}$ is the dimensionless temperature of the reservoir, T_o is the initial reservoir temperature (°C), T_i is the injection fluid temperature (°C), and T is the reservoir temperature (°C);

$\omega = \frac{(\rho C)_f Q}{4\pi b_m K_m}$ is the dimensionless convection parameter, $(\rho C)_f$ is the product of fluid density and fluid specific heat ($J/m^3°C$), Q is the constant injection rate (m^3/hr), b_m is the reservoir thickness (m) and K_m is the horizontal thermal conductivity in the reservoir ($w/m°C$);

$R = \frac{2r}{b_m}$ is the dimensionless radial distance and r is the radial distance from the well (m);

$\tau = \frac{4\alpha_m t}{b_m^2}$ is the dimensionless time, t is the time since injection started (hr) and α_m is the thermal diffusivity of the reservoir (m^2/hr);

$K = \frac{K_r}{K_m}$ is the dimensionless thermal conductivity and K_r is the vertical thermal conductivity of the caprock ($w/m°C$);

$\alpha = \left(\frac{\alpha_r}{\alpha_m}\right)^{1/2}$ is the dimensionless thermal diffusivity and α_r is the thermal diffusivity of the caprock (m^2/hr);

$\Gamma(\omega)$ is the Gamma function of ω; and

Erfc(x) is the Complementary Error function of x.

According to Avdonin (1964), the horizontal thermal conductivity in the caprock can be neglected for $\omega \geq 10$ and in the range of time from 0 to 6 years. However, when time equals infinity, Equation 1

gives U = 1, which implies that at steady state the temperature at every location in the reservoir is equal to the injected water temperature. Thus, the temperature distribution given by Equation 1 at steady state is unreal, and cannot be used.

Rubinshtein (1959) presented an analytical solution which allowed heat losses through the caprock. In this model, the horizontal and vertical heat conductions in both the reservoir and caprock, and heat convection in the reservoir were considered. Rubinshtein (1960) simplified his earlier model by neglecting the vertical heat conduction in the reservoir, and gave a solution for the temperature distribution in the reservoir. However, this solution was only valid for relatively small values of the convection parameter (ω). Rubinshtein (1963) developed another solution for relatively large values of the convection parameter (ω) to compliment his 1960 model.

Spillette (1965) indicated that all the previously discussed analytical models were subject to the assumptions that the fluid flow is one-dimensional and imcompressible, and the reservoir is homogeneous with constant physical properties. He developed a numerical model without using these assumptions to calculate the temperature distribution in the reservoir. He prepared curves of temperature versus radial distance using his model and compared them with the analytical solutions obtained by Lauwerier (1955) and Avdonin (1964). Spillette's comparison showed reasonable agreement among the three models. As a result, he concluded that the common assumptions made in the analytical models were reasonable.

Thomas (1967) gave three approximate methods for calculating the temperature distribution in a reservoir. These three approaches were applied to problems where the reservoir was relatively thin and the injection rate was relatively large. In Thomas's third method, the application of Schapery's (1962) direct method for approximating the inversion of Laplace transforms was illustrated. Thomas indicated that the use of Schapery's direct method yielded satisfactory results for the problems in his work.

Schapery (1962) proposed two methods for approximating the inversion of Laplace transforms; one of which is called the direct method. The direct method simply states that if $d[pF(p)]/d[\log(p)]$ is a slowly varying function of log p, then the inversion formula can be written as

$$f(t) \sim [F(p)]_{p=\frac{1}{2t}} \quad ,$$

where F(p) is the Laplace transform of f(t), p is the transform variable, and t is the original function variable.

Baker (1967) conducted experimental studies of the heat injection problem, and compared his experimental results with the analytical solutions obtained by Avdonin (1964), Lauwerier (1955) and Spillette (1965). Baker indicated that the assumption of no vertical temperature change in the reservoir appeared reasonable.

Evaluation of Aquifer Thermal Properties

Theis (1935) developed a mathematical model describing the problem

of radial flow to a well with a constant pumping rate in an extensive homogeneous and isotropic confined aquifer system. Theis (1935) obtained an analytical solution to this problem and proposed a graphical matching technique to determine two aquifer parameters from field observations of drawdown. Drawdown is defined as the difference between the initial piezometric head in the aquifer and the piezometric head in the aquifer at any given time after pumping test. The type curve is prepared by using the analytical solution. Superposition of the data curve onto the type curve makes it possible to find a match point. From this match point, values for the different variables are obtained, and the two aquifer parameters are uniquely determined.

To the same problem investigated by Theis (1935), Cooper and Jacob (1946) suggested a straight line approximation method for the determination of the two confined aquifer parameters. Chow (1952) developed a graphical method which was intended to take into account gradual changes in the aquifer parameters and avoid curve fitting. Kriz et al. (1966) also established a dimensionless type curve method for determining aquifer parameters.

To date, no information has been found on the use of graphical techniques for determining aquifer thermal properties. An analogy between fluid flow in aquifers and thermal flow in aquifers exists. Graphical procedures have been successfully developed for evaluating fluid flow parameters (Theis, 1935). Because of this success in fluid flow problems and the analogy between fluid flow and thermal flow, it is expected that graphical techniques can be developed for evaluating

the thermal properties of aquifers from field data.

Summary

From the previous review, the following results are important to the present study:

1 The assumption of an infinitly thick caprock is not accurate for all purposes in groundwater hydrology, and the effects of this assumption need additional study.

2 The assumption of no vertical temperature change in the aquifer (reservoir) appears reasonable for many groundwater problems.

3 The assumptions that the fluid flow is one-dimensional and incompressible, and that the aquifer is homogeneous with constant physical properties are widely accepted and used in groundwater studies.

4 The temperature of the individual sand grain is assumed to instantaneously become that of the fluid surrounding the sand grain.

5 In the aquifer, the horizontal heat conduction and heat convection caused by fluid movement are important.

6 In the caprock, horizontal heat conduction can be neglected during a limited period of time when the convection parameter is large. Vertical heat conduction in the caprock is significant and should be considered.

7 Schapery's (1962) direct method for approximating the inverse of Laplace transforms might be useful in this analytical work.

8 It should be possible to develop graphical techniques for determining thermal properties of aquifers using field measurements from thermal injection tests.

CHAPTER III

MATHEMATICAL REVIEW FOR THIS STUDY

In the present work, transcendental functions, Laplace transforms, and Laplace-Carson transforms are extensively used. Properties of each are introduced and discussed in the following three sections: (A) Transcendental Functions, (B) Laplace Transforms, and (C) Laplace-Carson Transforms.

Transcendental Functions

The hyperbolic cotangent function is an elementary transcendental function. It is customarily denoted by coth(x), where $x \in \mathbb{R}$ ($\mathbb{R}$ is the set of all real numbers). The definition of coth(x) is

$$\coth(x) = \frac{e^{x}+e^{-x}}{e^{x}-e^{-x}} \quad .$$

From the above definition, it is easy to show that coth(x) approaches unity when x is large. For example, when $x^2 \geq 10$, the difference between the true value of coth(x) and unity is less than 0.5 percent. The function coth(x) can also be represented (Abramowitz and Stegun, 1970) as an infinite series,

$$\coth(x) = \frac{1}{x} + \frac{x}{3} - \frac{x^3}{45} + \frac{2}{945}x^5 - \ldots. + \frac{2^{2n}B_{2n}x^{2n-1}}{(2n)!} + \ldots. \quad [2]$$

where B_{2n} is the $2n^{th}$ Bernoulli number and (2n)! is the factorial of

2n. When x is small coth(x) can be approximated by retaining only the first two terms in Equation 2. For example, when $x^2 \leq 1.0$ the error of truncating the series after the second term is less than 2.2 percent.

The Error function, denoted by Erf(x), is defined as

$$\mathrm{Erf}(x) = \frac{2}{\sqrt{\pi}} \int_0^x e^{-y^2}\, dy. \quad \ldots\ldots\ldots\ldots\ldots\ldots\ldots \quad [3]$$

The complementary error function, Erfc(x), is defined as 1 - Erf(x), and may be written as

$$\mathrm{Erfc}(x) = \frac{2}{\sqrt{\pi}} \int_x^\infty e^{-y^2}\, dy. \quad \ldots\ldots\ldots\ldots\ldots\ldots\ldots \quad [4]$$

The Gamma function is an important and fundamental higher transcendental function, which can be expressed several ways. For $x>0$ and $x \varepsilon \mathbb{R}$, Euler's integral for $\Gamma(x)$ is

$$\Gamma(x) = \int_0^\infty e^{-y} y^{x-1}\, dy. \quad \ldots\ldots\ldots\ldots\ldots\ldots\ldots \quad [5]$$

From Euler's integral representation, Equation 5, the incomplete Gamma function $\gamma(a,x)$ is defined as

$$\gamma(a,x) = \int_0^x e^{-y} y^{a-1}\, dy, \quad \ldots\ldots\ldots\ldots\ldots\ldots\ldots \quad [6]$$

and the complementary incomplete Gamma function, $\Gamma(a,x)$, is defined as

$$\Gamma(a,x) = \int_x^\infty e^{-y} y^{a-1}\, dy. \quad \ldots\ldots\ldots\ldots\ldots\ldots\ldots \quad [7]$$

The Gamma function is a meromorphic function (i.e. the function is analytical except for some poles), with poles at zero and all negative integers. When $x>0$, $\Gamma(x)$ is a rapidly-increasing function. Mathematically, this can easily be seen by evaluating its first derivative:

$$\Gamma'(n+1) = n!\log(n+1),$$

where the prime denotes the first derivative of $\Gamma(n+1)$ with respect to n, and n is any large positive integer. Numerically, this fact can best be understood by some practical values. For example $\Gamma(1)=1$, $\Gamma(10)=3.6288 \times 10^5$, $\Gamma(50)=6.10828 \times 10^{62}$, $\Gamma(59)=2.3505 \times 10^{78}$, and $\Gamma(100)=9.3326 \times 10^{155}$. Extensive numerical values of the Gamma function can be found in Ambramowitz and Stegun (1970).

The Gamma function has many special and nice properties. However, in this study, only the following two properties are used. They are

$$\Gamma(x)\Gamma(1-x) = \pi/\sin\pi x, \quad \ldots\ldots\ldots\ldots\ldots\ldots\ldots \quad [8]$$

and

$$\Gamma(x) = e^{-x}x^x\sqrt{\frac{2\pi}{x}}; \quad x \rightarrow \infty . \quad \ldots\ldots\ldots\ldots\ldots\ldots\ldots \quad [9]$$

Equation 9 is the well known Stirling formula for approximating the Gamma function.

The above material concerning the Gamma function can be found in many applied mathematics books, e.g. Henrici (1977), Olver(1974), Whittaker and Watson (1927), and Abramowitz and Stegun (1970).

There are many differential equations whose solutions can be expressed in terms of Bessel functions, another large and important family of transcendental functions. In this study, only the modified Bessel function of the first kind of order ν with parameter $\sqrt{\lambda}$, $I_\nu(\sqrt{\lambda}x)$, and the modified Bessel function of the second kind of order ν with parameter $\sqrt{\lambda}$, $K_\nu(\sqrt{\lambda}x)$, are used; where ν and $\sqrt{\lambda} \in \mathbf{R}$. A complete and imformative discussion of Bessel functions was given by Watson (1922).

The function $I_\nu(\sqrt{\lambda}x)$ can be expressed in an infinite series as

$$I_\nu(\sqrt{\lambda}x) = \sum_{m=0}^{\infty} \frac{(\frac{\sqrt{\lambda}x}{2})^{2m+\nu}}{m!\Gamma(m+1+\nu)}, \quad \nu \in \mathbf{R}. \quad \text{.....} \quad [10]$$

If ν is an integer, then $I_{-\nu}(\sqrt{\lambda}x) = I_\nu(\sqrt{\lambda}x)$. If ν is not an integer, then

$$I_{-\nu}(\sqrt{\lambda}x) = \sum_{m=0}^{\infty} \frac{(\frac{\sqrt{\lambda}x}{2})^{2m-\nu}}{m!\Gamma(m+1-\nu)}, \quad \nu > 0. \quad \text{.....} \quad [11]$$

The function $K_\nu(\sqrt{\lambda}x)$ can be expressed by the linear combinition of $I_\nu(\sqrt{\lambda}x)$ and $I_{-\nu}(\sqrt{\lambda}x)$ as

$$K_\nu(\sqrt{\lambda}x) = \frac{\pi}{2} \frac{I_{-\nu}(\sqrt{\lambda}x) - I_\nu(\sqrt{\lambda}x)}{\sin\pi\nu} \quad \text{.} \quad \text{.....} \quad [12]$$

If ν is an integer, Equation 12 assumes the indeterminate form 0/0; but by L'Hospital's rule a limit exists. This limit is lengthy and complex and is not reproduced here (the interested reader may refer to Wylie, 1960). The existence of the limit proves that $K_\nu(\sqrt{\lambda}x)$ is independent of $I_\nu(\sqrt{\lambda}x)$, even if ν is an integer (Wylie, 1960). Some properties of $I_\nu(\sqrt{\lambda}x)$ and $K_\nu(\sqrt{\lambda}x)$, $\nu \in \mathbb{R}$, which are used in this study are as follows.

From Equation 10, it is evident that the

$$\lim_{x\to\infty} I_\nu(\sqrt{\lambda}x) = \infty \text{ ,} \quad \lambda > 0 \text{ ;} \quad \text{.....} \quad [13]$$

while the

$$\lim_{x\to\infty} K_\nu(\sqrt{\lambda}x) = 0 \text{ .} \quad \text{.....} \quad [14]$$

As x approaches zero, only the first term in Equations 10 and 11 are needed to determine the value of $K_\nu(\sqrt{\lambda}x)$. Therefore, subsitituting the first term from Equations 10 and 11 into Equations 12 results in

$$\lim_{x\to 0} K_\nu(\sqrt{\lambda}x) = \lim_{x\to 0} \frac{\pi}{2} \frac{1}{\sin\pi\nu} \left\{ \frac{(\frac{\sqrt{\lambda}x}{2})^{-\nu}}{\Gamma(1-\nu)} - \frac{(\frac{\sqrt{\lambda}x}{2})^{\nu}}{\Gamma(1+\nu)} \right\} ,$$

or

$$\lim_{x\to 0} K_\nu(\sqrt{\lambda}x) = \frac{\pi}{2}\left(\frac{\sqrt{\lambda}}{2}\right)^{-\nu} \frac{1}{\Gamma(1-\nu)} \frac{1}{\sin(\pi\nu)} \lim_{x\to 0} x^{-\nu} \quad \ldots\ldots \quad [15]$$

The above equation indicates that $K_\nu(\sqrt{\lambda}x)$ is infinite at the origin. However, multiplying Equation 15 by x^ν gives

$$\lim_{x\to 0} x^\nu k_\nu(\sqrt{\lambda}x) = \frac{\pi}{2}\left(\frac{\sqrt{\lambda}}{2}\right)^{-\nu} \frac{1}{\sin(\pi\nu)} \frac{1}{\Gamma(1-\nu)} \quad .$$

The right hand side of this equation can be simplified by using the property of the Gamma function shown in Equation 8; which yields:

$$\lim_{x\to 0} x^\nu K_\nu(\sqrt{\lambda}x) = 2^{\nu-1} \lambda^{\frac{-\nu}{2}} \Gamma(\nu) \quad . \quad \ldots\ldots\ldots\ldots\ldots\ldots \quad [16]$$

There are various ways to represent $K_\nu(x)$ in integral form. One of them is (Watson, 1922)

$$K_\nu(x) = \frac{1}{2}\left(\frac{x}{2}\right)^\nu \int_0^\infty \exp\{-y - \frac{x^2}{4y}\} \frac{dy}{y^{1+\nu}} \quad .$$

By making a change in variable, $z = \frac{x^2}{4y}$, in the above equation, the following result is obtained,

$$K\nu(x) = \frac{1}{2}\left(\frac{4}{x^2}\right)^{\frac{\nu}{2}} \int_0^{\infty} \exp\{-z - \frac{x^2}{4z}\}\, z^{\nu-1}\, dz \quad ,$$

or

$$\int_0^{\infty} \exp\{-z - \frac{x^2}{4z}\}\, z^{\nu-1}\, dz = 2K\nu(x)\left(\frac{x^2}{4}\right)^{\nu/2} \quad . \quad \ldots\ldots\ldots \quad [17]$$

A large group of differential equations have their solutions expressed in terms of Bessel functions. This group of differential equations and the associated solutions can be generalized by the following theorem (Wylie, 1960):

Theorem 1. If $(1-a^2) \geq 4g$ and if neither d,f, nor q is zero, then, except in the case where it reduces to Euler's equation, the differential equation

$$x^2y'' + x(a + 2ex^f)y' + [g + dx^{2q} + e(a+f-1)x^f + e^2x^{2f}]y = 0 \quad ,$$

has the following complete solution:

$$y = x^{\mu}e^{-\beta x^f}\,[C_1 I\nu(\lambda x^q) + C_2 K\nu(\lambda x^q)] \quad ,$$

where $\mu = \frac{1-a}{2}$, $\beta = \frac{e}{f}$, $\lambda = \frac{\sqrt{|d|}}{q}$, $\nu = \frac{\sqrt{(1-a)^2 - 4g}}{2q}$, and $d<0$.

Laplace Transforms

Laplace transforms have been widely used to solve differential equations. To apply a Laplace transform to a function, the function must meet certain requirements so that an integral transform will exist (Sneddon, 1972). For most functions involved in engineering problems, Laplace transforms are applicable. In this study, the Laplace transform of $f(x,t)$ with respect to t is denoted as

$$L[f(x,t)] = F(x,p) \quad ,$$

where p is the transform variable, and the definition of $L[f(x,t)]$ is

$$L[f(x,t)] = \int_0^\infty e^{-pt} f(x,t)\, dt \quad .$$

In the above equation, the function e^{-pt} is called the kernel of the Laplace transform.

The following properties of Laplace transforms are directly verifiable from the integral definition of a Laplace transform. They are presented here without showing the detailed mechanics of the mathematical calculations.

For a function $f(x,t)$,

$$L\left[\frac{\partial f(x,t)}{\partial t}\right] = pF(x,p) - f(x,0), \quad \ldots\ldots\ldots\ldots\ldots\ldots \quad [18]$$

and

$$L\left[\frac{\partial^n f(x,t)}{\partial x^n}\right] = \frac{\partial^n F(x,p)}{\partial x^n} \quad , n = 1, 2, 3 \ldots . \quad \ldots\ldots \quad [19]$$

For a constant C,

$$L[C] = C/p \quad . \quad \ldots\ldots\ldots\ldots\ldots\ldots\ldots\ldots\ldots\ldots \quad [20]$$

The Laplace inversion of F(x,p) with respect to p is f(x,t), the original function. Customarily, this relation is expressed as

$$L^{-1}[F(x,p)] = f(x,t) \ .$$

When F(x,p) is prescribed, any formula enabling us to derive the form of the original function f(x,t) is called an inversion formula. Several inversion formulas are available for calculating the original functions. However, the use of these inversion formulas, except for simple functions, is extremely difficult and sometimes impossible. Fortunately, the original functions for a large number of Laplace transforms are available (i.e. Roberts and Kaufman, 1966; Bateman, 1953). By applying many operational laws, their applications can be extended.

If the original function of F(x,p) is f(x,t), then the change of scale law states that

$$L^{-1}[F(x,ap)] = \frac{1}{a}f(\frac{t}{a}) \ , \quad \ldots\ldots\ldots\ldots\ldots\ldots\ldots \quad [21]$$

and the translation law states that

$$L^{-1}[F(x,p+a)] = e^{-at}f(x,t) \ . \quad \ldots\ldots\ldots\ldots\ldots\ldots \quad [22]$$

If $L^{-1}[F(x,p)] = f(x,t)$ and $L^{-1}[G(x,p)] = g(x,t)$, then the convolution law states that

$$L^{-1}[F(x,p)G(x,p)] = \int_0^t F(x\ u)G(x,t-u)\ du \ . \quad \ldots\ldots\ldots \quad [23]$$

For the function, $F(x, p) = p^{\nu/2}K\nu(\lambda\sqrt{p})$, Carslaw and Jager (1959) give the inverse as:

$$L^{-1}[p^{\frac{\nu}{2}}K\nu(\lambda\sqrt{p})] = \frac{\lambda^{\nu}}{(2t)^{1+\nu}}\, e^{-\frac{\lambda^2}{4t}} \ . \quad \ldots\ldots\ldots\ldots\ldots\ldots \quad [24]$$

Laplace-Carson Transforms

As previously stated, the kernel of the Laplace transform is e^{-pt}. However, the Laplace-Carson transform has the kernel pe^{-pt}, thus, the definition of the Laplace-Carson transform of a function $f(x,t)$ with respect to t is

$$Lc[f(x\ t)] = \int_0^\infty pe^{-pt} f(x,t)\ dt = F(x,\ p) \quad .$$

The symbol Lc[f(x,t)] represents the Laplace-Carson transform of f(x,t) with respect to t.

From the definition of the Laplace-Carson transform; the following relationships are easily shown:

For a function f(x,t),

$$Lc\frac{[\partial f(x,t)]}{\partial t} = pF(x,p) - pf(x,0) \ , \quad \ldots\ldots\ldots\ldots\ldots \quad [25]$$

and

$$Lc\frac{[\partial^n f(x,t)]}{\partial x^n} = \frac{\partial^n F(x,p)}{\partial x^n} \ , \ n = 1,\ 2,\ 3 \ . \quad \ldots\ldots\ldots\ldots \quad [26]$$

For a constant C,

$$Lc[C] = C \ . \quad \ldots\ldots\ldots\ldots\ldots\ldots\ldots\ldots\ldots\ldots\ldots\ldots \quad [27]$$

Several similarities exist between the Laplace and Laplace-Carson transforms. However, the Laplace-Carson transform was particularly appropriate for solving one of the differential equations in this study. The following operational rules for the Laplace-Carson inversion (Ditkin and Kuznetsov, 1951) were used,

The Laplace-Carson inversion of F(p) is denoted as

$$Lc^{-1}[F(p)] = f(x) \quad .$$

Then,

$$Lc^{-1}\left[\frac{p}{p+\sqrt{p}} F(p+\sqrt{p})\right] = \int_0^x \frac{y}{2\sqrt{\pi(x-y)^3}} \exp\left[\frac{-y^2}{4(x-y)}\right] f(y)\, dy \quad . \qquad [28]$$

The change of scale law becomes

$$Lc^{-1}[F(ap)] = F\left(\frac{x}{a}\right) \quad . \quad \ldots\ldots\ldots\ldots\ldots\ldots\ldots\ldots \qquad [29]$$

Also,

$$Lc^{-1}[p^{\frac{\nu}{2}+1} K\nu(\lambda\sqrt{p})] = \frac{\lambda^{\nu} e^{\frac{-\lambda^2}{4x}}}{(2x)^{1+\nu}} \quad . \quad \ldots\ldots\ldots\ldots\ldots\ldots \qquad [30]$$

CHAPTER IV

DEVELOPMENT OF MATHEMATICAL MODELS

Two mathematical models of thermal injection into wells (Model I and Model II) are developed in this Chapter. Each is mathematically formulated in two sets of linear partial differential equations.

The two mathematical models only differ in the method used for thermal transfer into the caprock and bedrock. In Model I, the temperature distribution across a finitely thick caprock and bedrock is assumed to be linear. In Model II, this restrictive assumption is removed, and the temperature distribution across a finitely thick caprock and bedrock is allowed to be nonlinear.

A polar coordinate system is adopted, as shown in Figure 1. A few simplifying assumptions for this type of problem are made and listed below:

1 The aquifer is assumed to be horizontal and of uniform thickness b_m. The caprock and bedrock are impermeable to fluid flow and of finite thickness b_r. The system is symmetrical with respect to the midplane of the aquifer.

2 Flow is assumed to be steady. The injection rate Q is assumed to be constant. The injection well fully penetrates the aquifer.

3 The heat loss through the caprock and bedrock is governed by

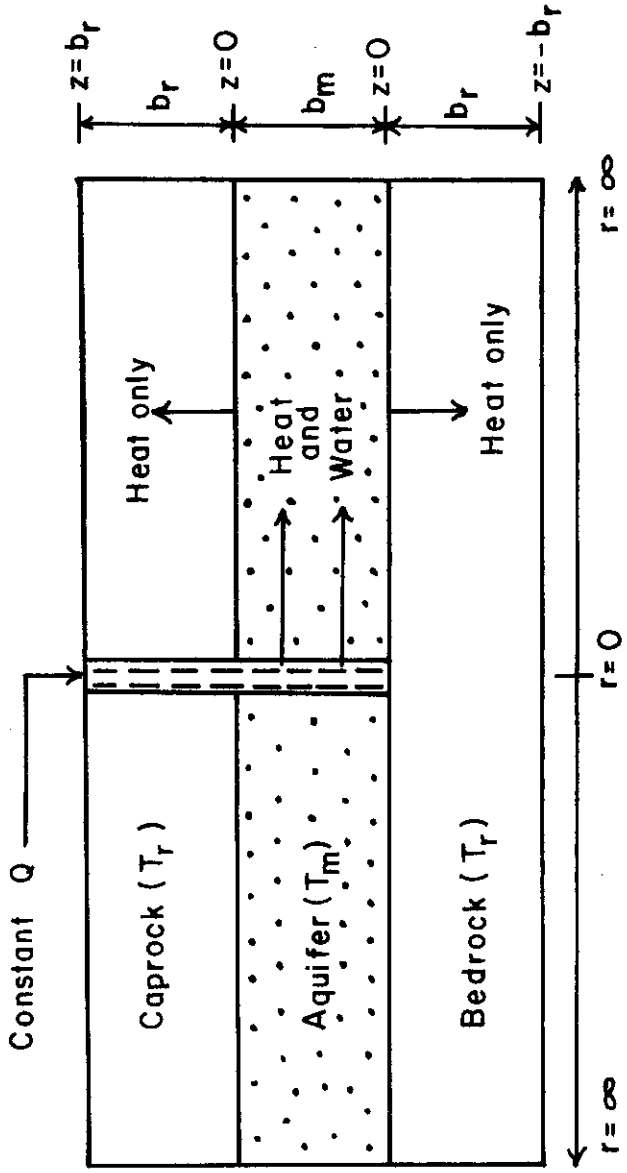

FIG. 1 Schematic of aquifer heat transfer model.

conduction in the vertical direction only, i.e., the horizontal thermal conductivity of the caprock and bedrock is assumed zero.

4 Heat transfer in the aquifer is governed by horizontal conduction and convection. The vertical temperature change is neglected in the aquifer, i.e., the vertical thermal conductivity in the aquifer is assumed infinite.

5 All the physical and thermal properties of the aquifer, caprock, and bedrock are assumed constant in time and space.

6 Convective heat transfer between the individual sand grains in the aquifer and the surrounding fluid is neglected, i.e., the sand grain instantaneously has the temperature of the surrounding fluid.

7 Initially, the water and sand in the aquifer, caprock and bedrock are at the same temperature T_i. The injected water is kept at a constant temperature T_o.

8 The temperature remains constant and equal to the initial temperature, T_i, at $z = \pm b_r$.

General Heat Equation in the Aquifer

In the aquifer, the solid phase refers to the sand or rock in the aquifer. The fluid phase exists in pores between the grains of sand or rock. Since heat conduction occures through both the solid phase and fluid phase of the aquifer, the thermal conductivity of the aquifer, K_m, is thus defined as

$$K_m = \phi K_f + (1 - \phi)K_s \quad , \quad \ldots\ldots\ldots\ldots\ldots\ldots\ldots \quad [31]$$

where ϕ is the porosity of the aquifer (dimensionless), and K_m, K_f and K_s are the thermal conductivities of the aquifer, fluid phase and solid phase, respectively, (w/m°C).

The thermal capacity of the aquifer is defined as

$$(\rho C)_m = \phi(\rho C)_f + (1 - \phi)(\rho C)_s \quad , \quad \ldots\ldots\ldots\ldots\ldots\ldots \quad [32]$$

where ρ is the density (Kg/m^3), C is the specific heat ($J/m^3°C$), and the subscripts m, f and s denote aquifer, fluid and solid,respectively.

The governing heat equation in the aquifer describes the heat transfer caused by horizontal conduction and convection in the aquifer, and heat losses by conduction across the caprock and bedrock. This equation is the same for both models. Applying the conservation of mass and energy principles, and using the assumptions previously stated, the resulting heat equation is:

$$\frac{\partial^2 T_m}{\partial r^2} + \frac{1 - 2\omega}{r}\frac{\partial T_m}{\partial r} + \frac{2K_r}{K_m b_m}\left.\frac{\partial T_r}{\partial z}\right|_{z=0} = \frac{1}{\alpha_m}\frac{\partial T_m}{\partial t} \quad , \quad \ldots\ldots\ldots \quad [33]$$

where all symbols have been previously defined. A detailed development of Equation 33 is given in Appendix A.

Partial Differential Equations For Model I

In addition to assumptions 1 through 8 on pages 25 and 27, Model I assumes that the temperature distribution across the caprock is linear. Considering the boundary conditions prescribed for the caprock, namely that $T_r(r, b_r, t) = T_o$ and $T_r(r, 0, t) = T_m$, the linear temperature distribution across the caprock is given by

$$T_r = (T_o - T_m) \frac{z}{b_r} + T_m \quad . \quad \ldots\ldots\ldots\ldots\ldots\ldots\ldots \quad [34]$$

Equation 34 is the temperature distribution function in the caprock. Because Equation 34 is linear, its derivative is

$$\left.\frac{\partial T_r}{\partial z}\right|_{z=0} = \frac{T_o - T_m}{b_r} \quad . \quad \ldots\ldots\ldots\ldots\ldots\ldots\ldots \quad [35]$$

Substituting Equation 35 into Equation 33, a condensed equation for Model I is

$$\frac{\partial^2 T_m}{\partial r^2} + \frac{1 - 2\omega}{r} \frac{\partial T_m}{\partial r} + \frac{2K_r(T_o - T_m)}{K_m b_m b_r} = \frac{1}{\alpha_m} \frac{\partial T_m}{\partial t} \quad , \quad \ldots\ldots\ldots \quad [36]$$

and

$$T_m(r, 0) = T_o \quad , \quad \ldots\ldots\ldots\ldots\ldots\ldots\ldots \quad [37]$$

$$T_m(0, t) = T_i \quad , \quad \ldots\ldots\ldots\ldots\ldots\ldots\ldots\ldots \quad [38]$$

$$T_m(\infty, t) = T_o \quad , \quad \ldots\ldots\ldots\ldots\ldots\ldots\ldots\ldots \quad [39]$$

where Equation 37 is the initial condition and Equations 38 and 39 are the two boundary conditions given for this model.

For simplicity, the dimensionless parameters, T, τ, R and K are introduced into Equations 36 through 39, yielding

$$\frac{\partial^2 T}{\partial R^2} + \frac{1 - 2\omega}{R} \frac{\partial T}{\partial R} - \xi T = \frac{\partial T}{\partial \tau} \quad , \quad \ldots\ldots\ldots\ldots\ldots\ldots \quad [40]$$

and

$$T(R, 0) = 0 \quad , \quad \ldots\ldots\ldots\ldots\ldots\ldots\ldots\ldots \quad [41]$$

$$T(0, \tau) = 1 \quad , \quad \ldots\ldots\ldots\ldots\ldots\ldots\ldots\ldots \quad [42]$$

$$T(\infty, \tau) = 0 \quad , \quad \ldots\ldots\ldots\ldots\ldots\ldots\ldots\ldots \quad [43]$$

where $\xi = \frac{K}{b}$ and $b = \frac{2b_r}{b_m}$ is the thickness ratio.

Partial Differential Equations For Model II

The limitation of the assumed linear temperature distribution across the caprock is removed in Model II. This does not affect the

heat equation developed for the aquifer; but the heat equation in the caprock is affected. According to the assumption that only vertical heat conduction occurs in the caprock, the governing heat equation in the caprock is the one-dimensional heat conduction equation

$$\frac{\partial^2 T_r}{\partial z^2} = \frac{1}{\alpha_r} \frac{\partial T_r}{\partial t} \quad , \quad \ldots\ldots\ldots\ldots\ldots\ldots\ldots\ldots\ldots\ldots \quad [44]$$

with

$$T_r(r, z, 0) = T_o \quad , \quad \ldots\ldots\ldots\ldots\ldots\ldots\ldots\ldots\ldots\ldots \quad [45]$$

$$T_r(r, 0, t) = T_m(r, t) \quad , \quad \ldots\ldots\ldots\ldots\ldots\ldots\ldots\ldots\ldots\ldots \quad [46]$$

and

$$T_r(r, b_r, t) = T_o \quad , \quad \ldots\ldots\ldots\ldots\ldots\ldots\ldots\ldots\ldots\ldots \quad [47]$$

where Equation 45 is the initial condition and Equations 46 and 47 are the two boundary conditions used in this model. Equations 44 through 47 fully describe the heat conduction problem in the caprock. A complete description of heat transfer for Model II is obtained by combining Equations 36 through 39 and Equations 44 through 47. Again, for simplicity, dimensionless parameters T, τ, R, K, α, b and $Z = 2z/b_m$ are introduced into Equations 36 through 39 and Equations 44 through 47. Consequently, Model II becomes:

$$\frac{\partial^2 T_1}{\partial Z^2} = \frac{1}{\alpha^2} \frac{\partial T_1}{\partial \tau} \quad , \quad \text{.....} \quad [48]$$

$$\frac{\partial^2 T}{\partial R^2} + \frac{1 - 2\omega}{R} \frac{\partial T}{\partial R} + K \frac{\partial T_1}{\partial Z}\bigg|_{Z=0} = \frac{\partial T}{\partial \tau} \quad , \quad \text{.....} \quad [49]$$

with

$$T_1(R, Z, 0) = 0 \quad , \quad \text{.....} \quad [50]$$

$$T_1(R, b, \tau) = 0 \quad , \quad \text{.....} \quad [51]$$

$$T_1(R, 0, \tau) = T(R, \tau) \quad , \quad \text{.....} \quad [52]$$

$$T(R, 0) = 0 \quad , \quad \text{.....} \quad [53]$$

$$T(0, \tau) = 1 \quad , \quad \text{.....} \quad [54]$$

$$T(\infty, \tau) = 0 \quad , \quad \text{.....} \quad [55]$$

and

$T_1 = \frac{T_r - T_o}{T_i - T_o}$ is the dimensionless caprock temperature.

CHAPTER V

RESULTS AND DISCUSSIONS

Model I is solved using Laplace transforms. Model II is solved using Laplace and Laplace-Carson transforms. Two asymptotic solutions for the unsteady state condition are obtained for Model II. One of the two asymptotic solutions is for long time periods, which is solved using Laplace transforms. The other asymptotic solution is for short time periods, which is solved using Laplace-Carson transforms. The solutions are in integral form and methods of numerical integration are discussed.

Analytical Solution For Model I

Model I was mathematically given by Equations 40 to 43, and for convenience these equations are reproduced here:

$$\frac{\partial^2 T}{\partial R^2} + \frac{1 - 2\omega}{R}\frac{\partial T}{\partial R} - \xi T = \frac{\partial T}{\partial \tau} \quad , \quad \ldots\ldots\ldots\ldots\ldots\ldots \quad [56]$$

$$T(R, 0) = 0 \quad , \quad \ldots\ldots\ldots\ldots\ldots\ldots \quad [57]$$

$$T(0, \tau) = 1 \quad , \quad \ldots\ldots\ldots\ldots\ldots\ldots \quad [58]$$

$$T(\infty, \tau) = 0 \quad . \quad \ldots\ldots\ldots\ldots\ldots\ldots \quad [59]$$

The Laplace transform is applied to $T(R, \tau)$ with respect to τ,

$$U(R, p) = L[T(R, \tau)] \quad .$$

Applying the relationships given in Equations 18, 19 and 57 to Equation 56 gives

$$\frac{d^2U}{dR^2} + \frac{1 - 2\omega}{R}\frac{dU}{dR} - \xi U = pU \quad . \qquad \text{[60]}$$

Equation 60 is a two-point boundary value problem. The two boundary conditions associated with Equation 60 are obtained by applying Laplace transforms to Equations 58 and 59, i.e.

$$U(0, p) = 1/p, \qquad \text{[61]}$$

and

$$U(\infty, p) = 0 \quad . \qquad \text{[62]}$$

The solution for the problem posed by Equations 60, 61 and 62 is

$$T = \frac{1}{\Gamma(\omega)} \int_u^\infty \exp(-x - \frac{\sigma}{x}) x^{\omega-1} \, dx \quad , \qquad \text{[63]}$$

where

$$u = \frac{R^2}{4\tau} = \frac{r^2}{4\alpha_m t} \quad , \quad \text{and}$$

$$\sigma = \frac{\xi R^2}{4} = \frac{r^2}{2b_r b_m} \frac{K_r}{K_m} \quad .$$

A detailed derivation of Equation 63 is given in Appendix B.

Equation 63 is the unsteady state solution for the aquifer temperature distribution for Model I. The unsteady state condition in engineering problems is time-dependent. The steady state condition is time-independent, and is theoretically approached as time approaches infinity.

In Equation 63, u is the only time-dependent parameter. When time equals infinity, u = 0. Hence, the steady state solution for the aquifer temperature distribution is

$$T = \frac{1}{\Gamma(\omega)} \int_0^\infty \exp(-x - \frac{\sigma}{x})\, x^{\omega-1}\, dx \quad . \quad \ldots\ldots\ldots\ldots\ldots \quad [64]$$

Equation 64 can be expressed in terms of a Bessel function. By comparing the integral on the right hand side of Equation 64 with Equation 17, it is found that

$$T = \frac{2\sigma^{\omega/2} K_\omega(2\sqrt{\sigma})}{\Gamma(\omega)} \quad . \quad \ldots\ldots\ldots\ldots\ldots\ldots\ldots\ldots \quad [65]$$

Equation 65 can also be obtained by solving the original differential equation (Equation 56), with $\partial T/\partial \tau = 0$.

In Equation 63, if r = 0, then u = σ = 0. This makes

$$T = \frac{1}{\Gamma(\omega)} \int_0^{\infty} \exp(-x) x^{\omega-1} \, dx \equiv 1 \quad ,$$

for the integral part of the above equation is by definition $\Gamma(\omega)$ (Equation 7). Thus the boundary condition at $r = 0$ is satisfied. If $r = \infty$, then $u = \sigma = \infty$. With both u and σ equal to infinity, the integral equals zero, and the other boundary condition is satisfied. The initial condition is easily checked by letting $t = 0$; then $u = \infty$, making the integral equal 0, and giving $T \equiv 0$. Furthermore, if the caprock is insulated and $K_r = 0$, then $\sigma = 0$, and

$$T = \frac{1}{\Gamma(\omega)} \int_u^{\infty} \exp(-x) x^{\omega-1} \, dx = \frac{\Gamma(\omega, u)}{\Gamma(\omega)} \quad .$$

In probability functions, $\Gamma(\omega, u)/\Gamma(\omega)$ is the cumulative Chi-Square distribution with degrees of freedom 2ω. (Abramowitz and Stegun, 1972). Therefore, if the caprock is insulated, the aquifer temperature distribution follows the cumulative Chi-Square distribution with degrees of freedom 2ω.

Analytical Solutions For Model II

The differential equations for Model II are:

$$\frac{\partial T_1}{\partial R^2} = \frac{1}{\alpha^2} \frac{\partial T_1}{\partial \tau} \quad , \quad \ldots\ldots\ldots\ldots\ldots\ldots\ldots\ldots\ldots\ldots \quad [66]$$

$$\frac{\partial^2 T}{\partial R^2} + \frac{1 - 2\omega}{R}\frac{\partial T}{\partial R} + K\frac{\partial T_1}{\partial Z}\bigg|_{Z=0} = \frac{\partial T}{\partial \tau} \quad , \quad \ldots\ldots\ldots\ldots\ldots \quad [67]$$

$$T_1(R, Z, 0) = 0 \quad , \quad \ldots\ldots\ldots\ldots\ldots\ldots\ldots\ldots \quad [68]$$

$$T_1(R, b, \tau) = 0 \quad , \quad \ldots\ldots\ldots\ldots\ldots\ldots\ldots\ldots \quad [69]$$

$$T_1(R, 0, \tau) = T(R, \tau) \quad , \quad \ldots\ldots\ldots\ldots\ldots\ldots\ldots \quad [70]$$

$$T(R, 0) = 0 \quad , \quad \ldots\ldots\ldots\ldots\ldots\ldots\ldots\ldots\ldots \quad [71]$$

$$T(0, \tau) = 1 \quad , \quad \ldots\ldots\ldots\ldots\ldots\ldots\ldots\ldots\ldots \quad [72]$$

and

$$T(\infty, \tau) = 0 \quad . \quad \ldots\ldots\ldots\ldots\ldots\ldots\ldots\ldots\ldots \quad [73]$$

Let

$$U_1(R, Z, p) = L[T_1(R, Z, \tau)] \quad ,$$

$$U(R, p) = L[T(R, \tau)] \quad .$$

Then the mathematical model is transformed to

$$\frac{d^2 U_1}{dZ^2} = p\frac{U_1}{\alpha^2} \quad , \quad \ldots\ldots\ldots\ldots\ldots\ldots\ldots\ldots\ldots \quad [74]$$

$$\frac{d^2U}{dR^2} + \frac{1 - 2\omega}{R}\frac{dU}{dR} + K\left.\frac{dU_1}{dZ}\right|_{Z=0} = pU \quad , \quad \text{.....} \quad [75]$$

$$U_1(R, b, p) = 0 \quad , \quad \text{.....} \quad [76]$$

$$U_1(R, 0, p) = U(R, p) \quad , \quad \text{.....} \quad [77]$$

$$U(0, p) = 1/p \quad , \quad \text{.....} \quad [78]$$

and

$$U(\infty, p) = 0 \quad . \quad \text{.....} \quad [79]$$

Equation 74 is solved first, then Equation 75 is subsequently solved. The solution of the two-point boundary value problem posed by Equations 74, 76 and 77 is (Sneddon, 1972)

$$U_1 = U\frac{\sinh[(b - z)\sqrt{p}/\alpha]}{\sinh[b\sqrt{p}/\alpha]} \quad . \quad \text{.....} \quad [80]$$

Thus

$$\left.\frac{dU_1}{dZ}\right|_{Z=0} = -\frac{\sqrt{p}}{\alpha}\coth\left(\frac{b\sqrt{p}}{\alpha}\right) U \quad .$$

Placing the above result into Equation 75 gives

$$\frac{d^2U}{dR^2} + \frac{1 - 2\omega}{R}\frac{dU}{dR} - \left[p + \frac{K\sqrt{p}}{\alpha}\coth\left(\frac{b}{\alpha}\sqrt{p}\right)\right]U = 0 \quad . \quad \ldots\ldots \quad [81]$$

Following the detailed derivation given in Appendix B, the solution to Equations 81, 78 and 79 is

$$U = \frac{2^{1-\omega}R^{\omega}}{\Gamma(\omega)}\frac{\chi^{\omega/2}K_{\omega}(\sqrt{\chi}R)}{p} \quad , \quad \ldots\ldots\ldots\ldots\ldots\ldots \quad [82]$$

where

$$\chi = p + \frac{K\sqrt{p}}{\alpha}\coth\left(\frac{b\sqrt{p}}{\alpha}\right) \quad . \quad \ldots\ldots\ldots\ldots\ldots\ldots \quad [83]$$

The inversion of Equation 82 is difficult by any known inversion formulas. However, approximate solutions, one for sufficiently short time periods and the other for sufficiently long time periods, can be obtained.

The parameters (τ and p) in the Laplace transform are inversely related. Thus, as τ becomes small, p becomes large. The solution for short time periods is obtained from Equation 82 when p becomes large. When p is large the argument of the hyperbolic cotangent in Equation 83 approaches unity. As discussed in Chapter III, for $b^2p/\alpha^2 \geq 10$, the hyperbolic cotangent may be replaced by unity without appreciably changing the value of Equation 82. Using this approximation, Equation 82 is written as

$$U = \frac{2^{1-\omega} R^{\omega}}{\Gamma(\omega)} \frac{(p + \frac{K}{\alpha}\sqrt{p})^{\omega/2} \; K_{\omega}(R\sqrt{p + \frac{K}{\alpha}\sqrt{p}})}{p} \quad . \quad \ldots\ldots\ldots \quad [84]$$

Even with this approximation, no inversion formula to Equation 84 in Laplace transforms was found. Instead, Laplace-Carson transforms were used to solve this problem. The derivation of the solution for short time periods using Laplace-Carson transforms is given in Appendix C. The solution is

$$T = \frac{1}{\Gamma(\omega)} \int_{u}^{\infty} e^{-x} \mathrm{Erfc}\left[\frac{\eta\sqrt{u}}{\sqrt{x(x-u)}}\right] x^{\omega-1} dx \quad , \quad \ldots\ldots\ldots\ldots \quad [85]$$

where

$$\eta = \frac{KR}{4\alpha} = \frac{1}{2} \frac{r}{b_m} \frac{K_r}{K_m} \left(\frac{\alpha_m}{\alpha_r}\right)^{1/2} \quad .$$

The time criterion for short time periods is $\eta \leq 0.1 \; b^2/\alpha^2$ or $t \leq 0.1 \; b_r^2/\alpha_r$.

Making the change of variable, $y = \frac{u}{x}$, in Equation 85 results in

$$T = \frac{u^{\omega}}{\Gamma(\omega)} \int_0^1 \exp\left(\frac{-u}{y}\right) \mathrm{Erfc}\left[\frac{\eta y}{\sqrt{u(1-y)}}\right] \frac{dy}{y^{1+\omega}} \quad .$$

Substituting $u = \frac{R^2}{4\tau}$ and $\eta = \frac{KR}{4\alpha}$ into the above equation gives

$$T = \frac{1}{\Gamma(\omega)}\left(\frac{R^2}{4}\right)^{\omega}\int_0^1 \exp\left(\frac{-R^2}{4\tau y}\right)\ \mathrm{Erfc}\left(\frac{K\sqrt{\tau}}{2\alpha}\ \frac{y}{\sqrt{1-y}}\right)\ \frac{dy}{y^{1+\omega}} \quad ,$$

which is identical with the solution of Avdonin (1964), which was given in Equation 1. Recalling that Avdonin assumed the caprock thickness to be infinite while Equation 85 assumes a finite caprock thickness, then it can be concluded that the caprock thickness, b_r, is not important for short time periods where $t \leq 0.1\ b_r^2/\alpha_r$.

The parameter b_r is not directly involved in the solution of Equation 85, but appears only in the time criterion inequality, $t \leq 0.1\ b_r^2/\alpha_r$. This indicates that the thermal response in the aqufier for some time period after injection starts is independent of the caprock thickness. The duration of this time period is proportional to the square of the caprock thickness. Therefore, the larger b_r is, the longer Equation 85 is applicable.

In Figure 2, Equation 85 is graphically presented for different values of ω with η equal to 0.5. Note that the thermal front extends further for larger values of ω. Physically, a larger injection rate will increase ω, and accelerate the movement of the thermal front because more heat is added to the aquifer. On the other hand, a thinner aquifer will also increase ω. A thin aquifer has less aquifer volume per unit radius than a thick aquifer, and will absorb less heat; thus the thermal front will extend further for a thin aquifer (all the properties being equal).

In Figure 3, Equation 85 is graphically presented for different values of η with ω equal to 90. The parameter η is a combination of the thermal properties K/α and geometric distance R. A larger vertical thermal conductivity in the caprock makes η larger; consequently more heat is lost through the caprock and the thermal front does not advance as far. This explains why the curves with larger values of η always have smaller values of T.

If $r = 0$, then $u = 0$ and the argument of the Complementary Error function in Equation 85 is zero. Since $\text{Erfc}(0) = 1$, Equation 85 becomes

$$T = \frac{1}{\Gamma(\omega)} \int_0^{\infty} e^{-x} x^{\omega-1} \, dx \equiv 1 \quad ,$$

when $r = 0$.

In the cases where either $r = \infty$ or $t = 0$, the integrand of Equation 85 exists, and the value of u is infinity. Under this condition, Equation 85 yields $T \equiv 0$. These three cases prove that Equation 85 satisfies the initial and boundary condition prescribed for this problem.

By letting $t = \infty$ ($u = 0$), Equation 85 yields the steady state temperature distribution, $T \equiv 1$. However, to apply Equation 85, the time criterion, $t \leq 0.1 \, b_r^2/\alpha_r$, must be met. This indicates that Equation 85 should not be used to evaluate steady state temperature distributions.

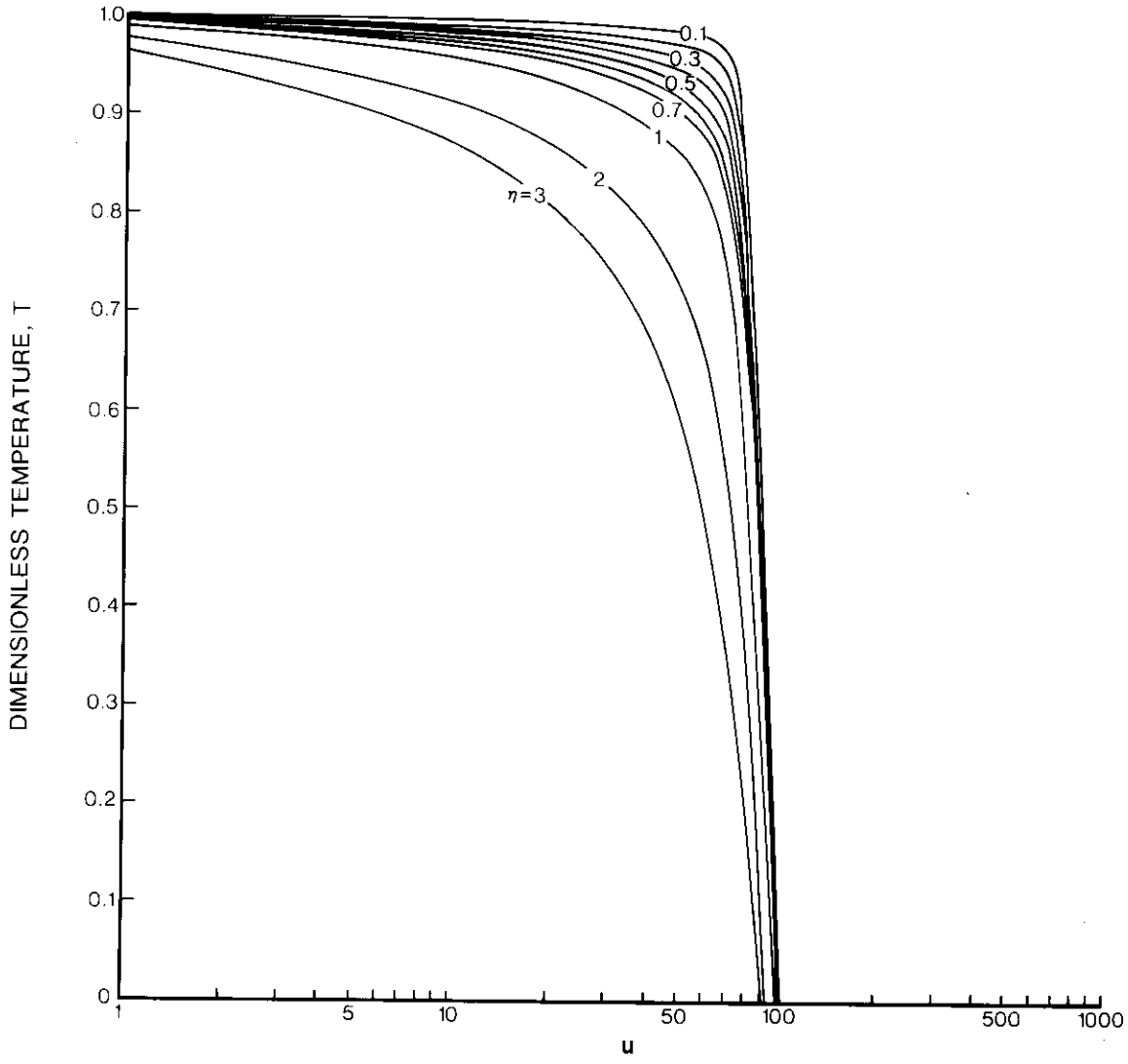

FIG. 3 Type curves for short time period solution (ω=90).

A solution for long time periods corresponds to that obtained from Equation 82 if p becomes small (τ becomes large). When $b^2p/\alpha^2 \leq 1.0$, the hyperbolic contangent in Equation 83 can be approximated by $\alpha/b\sqrt{p} + b\sqrt{p}/3\alpha$. Making this substitution for $\coth(b\sqrt{p}/\alpha)$ in Equation 83 gives

$$\chi = \xi + \delta' p \quad , \quad \ldots\ldots\ldots\ldots\ldots\ldots\ldots\ldots\ldots\ldots \quad [86]$$

where

$$\delta' = 1 + \delta \quad , \text{ and}$$

$$\delta = \frac{Kb}{3\alpha^2} = \frac{2}{3}\frac{b_r}{b_m}\frac{(\rho C)_r}{(\rho C)_m} \quad .$$

Using χ as defined in Equation 86, Equation 82 is simplified to:

$$U = \frac{2^{1-\omega}R^{\omega}}{\Gamma(\omega)} \frac{(\delta' p + \xi)^{\omega/2} K_{\omega}(R\sqrt{\delta' p + \xi})}{p} \quad . \quad \ldots\ldots\ldots\ldots \quad [87]$$

A detailed derivation of the inversion of Equation 87 is given in Appendix B. The result is

$$T = \frac{1}{\Gamma(\omega)} \int_{(1+\delta)\,u}^{\infty} \exp(-x - \frac{\sigma}{x})\, x^{\omega-1}\, dx \quad . \quad \ldots\ldots\ldots\ldots \quad [88]$$

Equation 88 is the aquifer temperature distribution for long time periods, $\tau \geq b^2/\alpha$ or $t \geq b_r^2/\alpha_r$. For Equation 88 to be applicable, the time parameter τ must be greater than or equal to the lower limit,

b^2/α. No upper limit exists. Thus τ can increase to infinity, yielding a steady state solution for finitely thick caprocks. The only time-dependent parameter in Equation 88 is u. Therefore, as $\tau \to \infty$, $u \to 0$ and the steady state solution is

$$T = \frac{1}{\Gamma(\omega)} \int_0^{\infty} \exp(-x - \frac{\sigma}{x})\, x^{\omega-1}\, dx \quad ,$$

which is identical with Equation 64, the steady state solution obtained for Model I. Thus, the steady state solutions are the same for both models. Comparing the unsteady state solution for long time periods in Model II (Equation 88) with the unsteady state solution in Model I (Equation 63)it is found that the only difference between them is the lower limit of the integral; namely, $(1+\delta)u$ for Equation 88 and u for Equation 63. Apparently, in Model I the parameter δ is zero. The parameter δ being zero could result from a relatively small caprock thickness (b_r) or large aquifer thickness(b_m). Under these conditions, Model II for long time period essentially equals Model I and the assumption in Model I of a linear temperature distribution in the caprock appears valid.

In Figure 4, Equation 64 is graphically presented for different values of ω. At steady state, a larger ω gives a larger value of T at a fixed point in the aquifer. Also, a larger value of ω makes the thermal front in the aquifer move a greater distance.

In Figure 5, Equation 88 is graphically presented for different values of ω with σ equal to 10.0. As previously discussed, larger

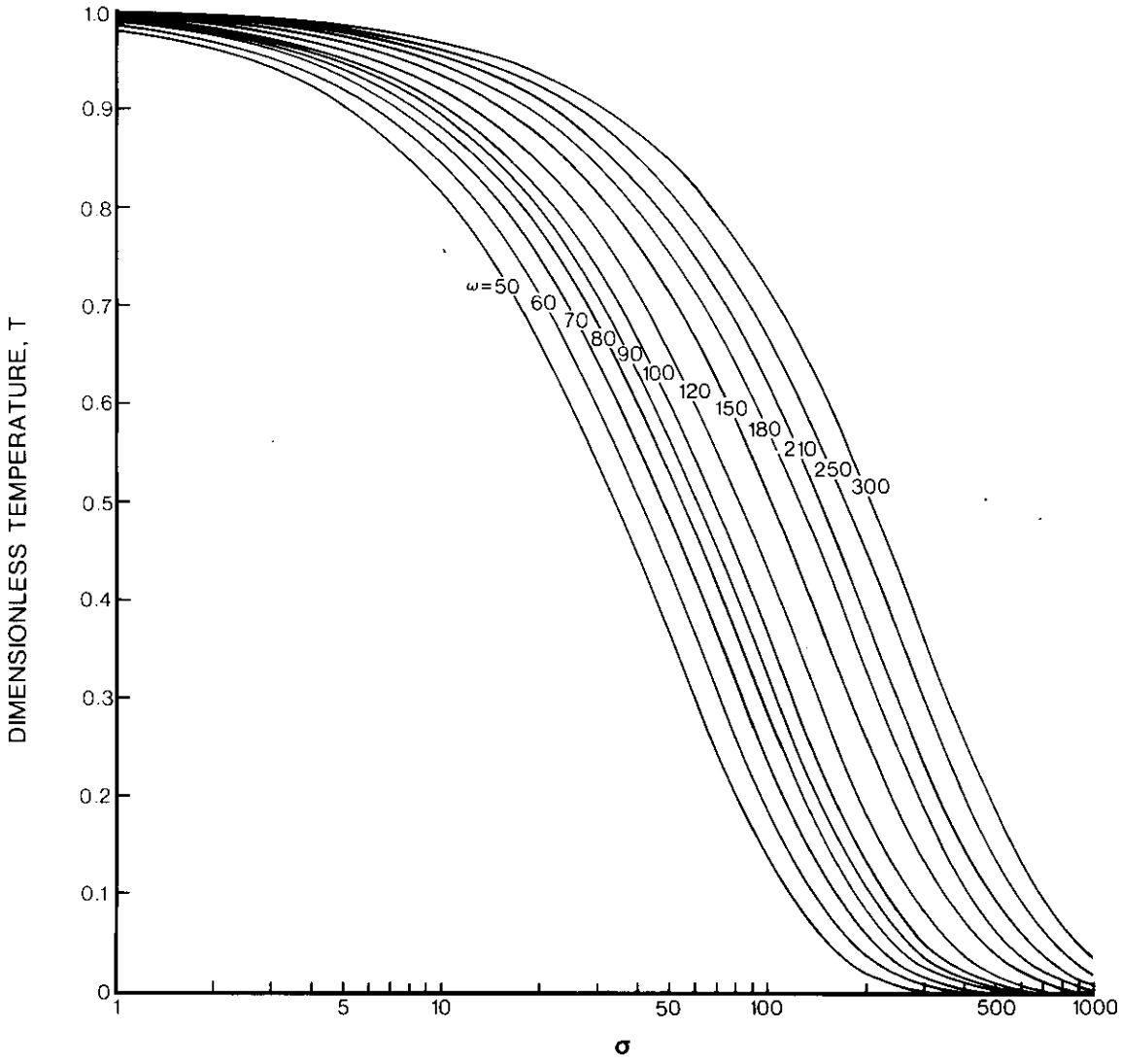

FIG. 4 Type curves for steady state solution.

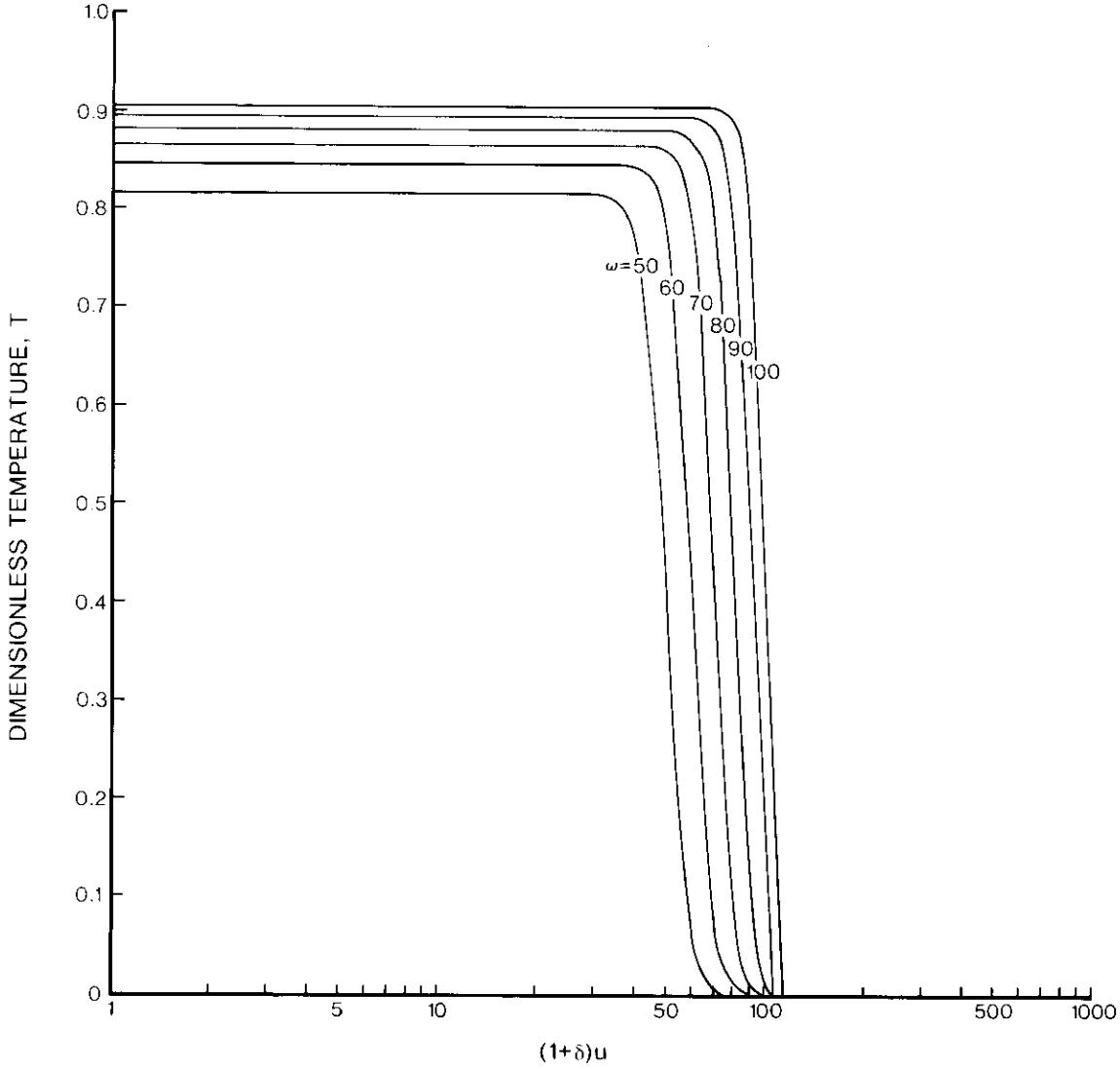

FIG. 5 Type curves for long time period solution (σ=10).

values of ω yield larger values of T at a fixed point in the aquifer, and the thermal front extends a greater distance.

In Figure 6, Equation 88 is graphically presented for different values of σ with ω equal to 90.0. Mathematically, a large value of σ makes the integrand in Equation 88 smaller, consequently a smaller value of T. Physically, a larger value of σ results from a larger value of K_r. When K_r is large, more heat is lost through the caprock, and less heat is available for transportation through the aquifer.

Numerical Integration of Solutions

The integrals appearing in the above solutions are not solvable by ordinary means of integration. Accordingly, it was necessary to use numerical methods. When a definite integral is to be evaluated by numerical methods, it is essential that the integrand have no sigularities in the domain of interest. This requirement is satisfied by each of the previously given solutions.

In groundwater hydrology, values of ω usually range from 50 to 250. For such large values of ω, $\Gamma(\omega)$ is an extremely large number, and is not manageable by most digital computers. However, the Binet formula (Whittaker and Watson, 1927) gives an expression for log $\Gamma(x)$, which reduces $\Gamma(x)$ to smaller and more manageable values. In numerical libraries(IBM System/360 Scientific Subroutine Package), the Binet foumula for log $\Gamma(x)$ is given in the subroutine entitled DLGAM, which computes the natural lognithm of the Gamma function of a given argument, x, where $10^{-9} < x < 10^{70}$.

To use ln $\Gamma(x)$,determined by DLGAM, to evaluate the solution integrals, the integrands must be modified. Using the steady state solution,as an example, the integrand used for numerical integration may be expressed as

$$\frac{1}{\Gamma(\omega)} \int_0^\infty \exp(-x - \frac{\sigma}{x})\, x^{\omega-1}\, dx =$$

$$\int_0^\infty \exp[-x - \frac{\sigma}{x} + (\omega-1)\ln(x) - \ln\Gamma(\omega)]\, dx \quad .$$

Using this transformation not only overcomes the exponetial overflow problem of $\Gamma(\omega)$, but also makes the integral numerically much smaller; so that it can be numerically evaluated on digital computers.

Gaussian quadrature formulas are approporiate for numerically integrating the solutions. However, Gaussian quadrature was developed to evaluate integrals with finite integration intervals. Although several methods are available for transforming an infinite integration interval into a finite interval, the following method was found effective for these problems.

All the solution integrands have a common form

$$f(x) = e^{-x}\, x^{\omega-1}\, g(x) \quad ,$$

where $g(x) = \mathrm{Erfc}[\frac{\eta\sqrt{u}}{\sqrt{x(x-u)}}]$ for the short time period solution, and

$g(x) = e^{-\sigma/x}$ for the remaining solutions. In both cases, $g(x) \leq 1$. Thus,

$$\frac{1}{\Gamma(\omega)} \int_u^\infty e^{-x} x^{\omega-1} g(x)\, dx \leq \frac{1}{\Gamma(\omega)} \int_u^\infty e^{-x} x^{\omega-1} dx \quad .$$

Making a change of variable, $y = \frac{1}{x}$, the right hand side of the above inequality results in

$$\frac{1}{\Gamma(\omega)} \int_u^\infty e^{-x} x^{\omega-1} dx = \frac{1}{\Gamma(\omega)} \int_0^{\frac{1}{u}} e^{-\frac{1}{y}} \frac{dy}{y^{1+\omega}} \quad ,$$

and

$$\frac{1}{\Gamma(\omega)} \int_0^{\frac{1}{u}} e^{-\frac{1}{y}} \frac{dy}{y^{1+\omega}} = \frac{1}{\Gamma(\omega)} \int_0^\varepsilon \frac{e^{-1/y} dy}{y^{1+\omega}} + \frac{1}{\Gamma(\omega)} \int_\varepsilon^{\frac{1}{u}} \frac{e^{-1/y} dy}{y^{1+\omega}} \quad .$$

A value for ε must be found so that the first integral on the right hand side of the above equation may be neglected. It is apparent that

$$\frac{1}{\Gamma(\omega)} \int_0^\varepsilon e^{-1/y} \frac{dy}{y^{1+\omega}} \leq \frac{\varepsilon}{\Gamma(\omega)} e^{-1/\varepsilon} \frac{1}{\varepsilon^{1+\omega}} \quad .$$

Introducing the Stirling formula, given in Equation 9, into the above inequality results in

$$\frac{1}{\Gamma(\omega)} \int_0^{\varepsilon} e^{-1/y} \frac{dy}{y^{1+\omega}} \leq \sqrt{\frac{\omega}{2\pi}}\, e^{-1/\varepsilon} \left(\frac{e}{\varepsilon\omega}\right)^{\omega} \quad .$$

The term $\sqrt{\frac{\omega}{2\pi}}\, e^{-1/\varepsilon} \left(\frac{e}{\varepsilon\omega}\right)^{\omega}$ in the above inequality is the estimated error of neglecting the integral from zero to ε. In the field of groundwater hydrology, the value of ω usually falls within the range of $50 \leq \omega \leq 250$. Therefore, using the Stirling formula to approximate $\Gamma(\omega)$ appears to be reasonable. The value of ε can now be determined from the estimated error term, $\sqrt{\frac{\omega}{2\pi}}\, e^{-1/\varepsilon} \left(\frac{e}{\varepsilon\omega}\right)^{\omega}$. For example, if $\omega = 100$, and choose $\varepsilon = \frac{1}{2\omega}$, then the error due to neglecting the integral from 0 to ε is at worst 7.50536×10^{-13}. The error becomes even smaller as ω becomes larger.

However, the error estimated here is for the transformed variable, $y = 1/x$. For the original integral,

$$\frac{1}{\Gamma(\omega)} \int_u^{\infty} e^{-x} x^{\omega-1} g(x)dx \leq \frac{1}{\Gamma(\omega)} \int_u^{1/\varepsilon} e^{-x} x^{\omega-1} dx + \frac{1}{\Gamma(\omega)} \int_{1/\varepsilon}^{\infty} e^{-x} x^{\omega-1} dx \quad ,$$

and the term $\sqrt{\frac{\omega}{2\pi}}\, e^{-1/\varepsilon} \left(\frac{e}{\varepsilon\omega}\right)^{\omega}$ is used to estimate the error when the original integral from $1/\varepsilon$ to ∞ is neglected. Thus, the integration interval $(u, 2\omega)$ may be used to approximate the integration integral (u, ∞) without any appreciably error when values of $\omega \geq 50$ are used.

From this analysis, the problem of a non-finite integration interval is overcome, and Gaussian quadrature becomes applicable. The unsteady state solutions are numerically evaluated by Gaussian quadature over the integration interval u to 2.0ω.

The steady state solution is evaluated using the following method. Applying the change of variable, $y = 1/x$, to the steady state solution, the following equation is obtained:

$$\frac{1}{\Gamma(\omega)} \int_0^\infty \exp(-x - \frac{\sigma}{x}) x^{\omega-1} dx = \frac{1}{\Gamma(\omega)} \int_0^\infty \exp(-\sigma y - \frac{1}{y}) \frac{dy}{y^{1+\omega}} =$$

$$\frac{1}{\Gamma(\omega)} \{ \int_0^\infty \frac{\exp(-\frac{1}{y})}{y^{1+\omega}} dy - \int_0^\infty \frac{\exp(-\frac{1}{y}) - \exp(-\sigma y - \frac{1}{y})}{y^{1+\omega}} dy \} =$$

$$1 - \frac{1}{\Gamma(\omega)} \int_0^\infty \frac{\exp(-\frac{1}{y}) - \exp(-\sigma y - \frac{1}{y})}{y^{1+\omega}} dy \quad , \quad \ldots\ldots\ldots\ldots \quad [89]$$

where

$$\int_0^\infty \frac{\exp(-\frac{1}{y})}{y^{1+\omega}} dy = \Gamma(\omega) \quad .$$

Two advantages are gained in this way: (1) the integrand

$\frac{\exp(-\frac{1}{y}) - \exp(-\sigma y - \frac{1}{y})}{\Gamma(\omega) y^{1+\omega}}$ is numerically much smaller; and (2) the

numerical accuracy is improved considerably. The original integration interval is also changed from $(0, \infty)$ to $(0, 2.0\omega)$, so that Gaussian quadrature can be applied.

In summary, Gaussian quadrature is used to numerically integrate the solutions from u or zero to 2ω, rather than from u or zero to ∞. The $\ln \Gamma(x)$, determined by DLGAM, is also used to prevent exponential overflow problem. Results obtained using these procedures are shown in Figures 2, 3, 4, 5 and 6. The computer programs used to obtain the solutions are given in Appendix D.

Approximate Solution For Laplace Inversions

In this study, temperature distributions for intermediate ranges of time, $0.1 \frac{b_r^2}{\alpha_r} \leq t \leq \frac{b_r^2}{\alpha_r}$, are approximated using Schapery's (1962) method. According to Schapery's direct method (1962),

$$T = \frac{2^{1-\omega} R^{\omega}}{\Gamma(\omega)} \chi_1^{\frac{\omega}{2}} K\omega(R\sqrt{\chi_1}) \quad , \quad \ldots\ldots\ldots\ldots\ldots\ldots\ldots \quad [90]$$

where

$$\chi_1 = \frac{1}{2\tau} + \frac{K}{\alpha} \frac{1}{\sqrt{2\tau}} \coth\left(\frac{b}{\alpha} \frac{1}{\sqrt{2\tau}}\right) \quad .$$

From Equation 17, Equation 90 may be expressed in integral form as

$$T = \frac{1}{\Gamma(\omega)}\int_0^{\infty} \exp\{-z - \frac{R^2\chi_1}{4z}\}\ z^{\omega-1}dz \quad . \quad \ldots\ldots\ldots\ldots\ldots \quad [91]$$

Equation 91 is evaluated using the numerical technique developed for the steady state solution. In Figure 7, results from Equation 91 are compared with those of Equation 85 for $\tau \leq 0.1\ b^2/\alpha^2$, and of Equation 88 for $\tau \geq b^2/\alpha^2$. Apparently, the approximate method of Schapery yields satisfactory results only for large times, and its use is not recommended for problems of this nature unless some error in the solution can be accepted.

Summary

Solutions for the two models are summarized below:

1 The unsteady state aquifer temperature distribution for Model I is

$$T = \frac{1}{\Gamma(\omega)} \int_u^{\infty} \exp(-x - \frac{\sigma}{x})\ x^{\omega-1}dx \quad .$$

2 The unsteady state aquifer temperature distribution for short time periods, $t < 0.1b_r^2/\alpha_r$, in Model II is

$$T = \frac{1}{\Gamma(\omega)} \int_u^{\infty} e^{-x}\mathrm{Erfc}(\frac{\eta\sqrt{u}}{\sqrt{x(x-u)}})\ x^{\omega-1}dx \quad .$$

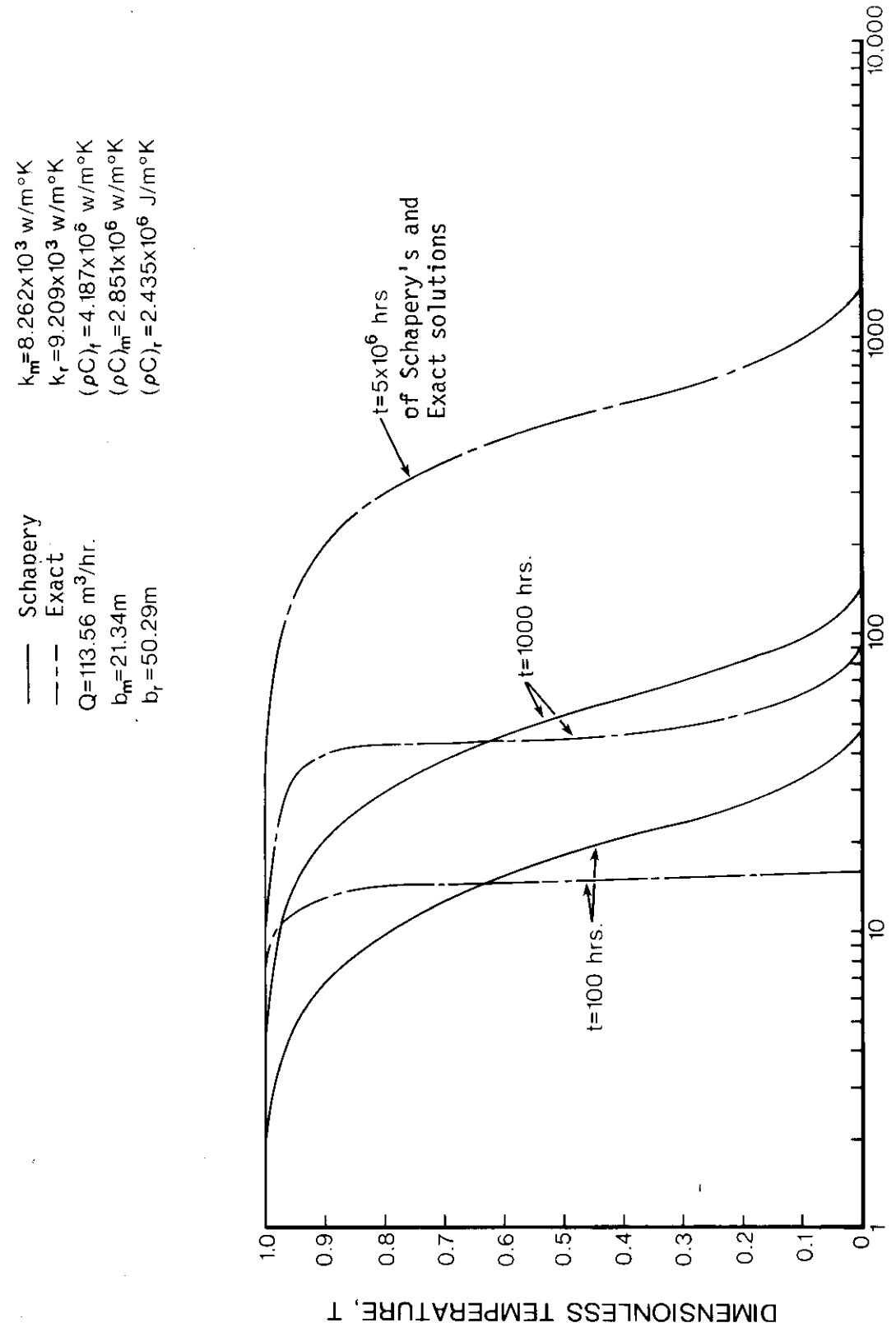

FIG. 7 Comparision of Schapery's approximate solution with exact solution.

3 The unsteady state aquifer temperature distribution for long time periods, $t \geq b_r^2/\alpha_r$, in Model II is

$$T = \frac{1}{\Gamma(\omega)} \int_{(1+\delta)u}^{\infty} \exp(-x - \frac{\sigma}{x})\, x^{\omega-1} dx \quad .$$

4 The steady state aquifer temperature distribution for both models is

$$T = \frac{1}{\Gamma(\omega)} \int_{0}^{\infty} \exp(-x - \frac{\sigma}{x})\, x^{\omega-1} dx$$

or

$$T = \frac{2\sigma^{\frac{\omega}{2}} K_{\omega}(2\sqrt{\sigma})}{\Gamma(\omega)} \quad .$$

CHAPTER VI

GRAPHICAL TECHNIQUES TO EVALUATE AQUIFER THERMAL PROPERTIES

In the present study, four pertinent thermal properties, K_r, K_m, $(\rho C)_r$ and $(\rho C)_m$, are needed to operate the models. These parameters are difficult to evaluate under field conditions. Using the previously developed solutions, a curve matching technique is proposed for estimating the four thermal properties using field data. The values of K_r and K_m are determined using field data collected near steady state conditions. The values of $(\rho C)_r$ and $(\rho C)_m$ are determined using field data measured soon after injection starts. Since the steady state condition is difficult to attain in the field, an approximate graphical technique for evaluating the parameters is developed without using the steady state data. In this approximate method, K_m is assumed equal to K_r, and $(\rho C)_r$ is assumed equal to $(\rho C)_m$.

Illustration of the Graphical Technique

1 Prepare a set of dimensionless-type curves from the steady state solution (hereafter referred to as the steady state type curves). Steady state type curves are constructed such that T versus the logarithm of σ. Each single curve corresponds to a particular value of ω.

2 Temperature observations from several wells at different

radii from the injection well and approaching steady state are plotted as T versus the logarithm of $r^2/b_m b_r$ (hereafter) referred to as the steady state field curve).

3 Superimpose the steady state field curves onto the steady state type curves, keeping the coordinate axes parallel and the logarithmic axes the same until a matching position is obtained between the steady state field curve and one of the steady state-type curves. In some cases, interpolation between two curves may be necessary. Because each steady state type curve has a unique value of ω, the value of K_m can be calculated from the following equation:

$$\omega = \frac{(\rho C)_f Q}{4\pi b_m K_m} \quad .$$

4 In the matching position, select an arbitrary value of σ and its associated value of $r^2/b_r b_m$ from the steady state field curve. Since

$$\sigma = \frac{r^2}{2b_r b_m} \frac{K_r}{K_m} \quad ,$$

and K_m is known from step 3, the value of K_r can be calculated.

5 With ω known, a set of unsteady state type curves are constructed using the solution for short time periods from Model II. The curves are plotted such that T versus the logarithm of u, and each curve is associated with a particular value

of η, while ω is held constant.

6 Field data from any one of the observation wells at an early time is plotted such that T versus the logarithm of r^2/t (hereafter referred to as the unsteady state field curves).

7 Superimpose the unsteady state field curves onto the unsteady state type curves, keeping the coordinate axes parallel and the logarithmic axes the same. The field data curve is matched with one of the unsteady state type curves. Select an arbitrary value of r^2/t from the field curves and a corresponding value of u from the type curve. The value of α_m can then be calculated from the following equation:

$$\alpha_m = \frac{r^2}{4ut} \quad .$$

After α_m is determined, the value of $(\rho C)_m$ is determined using

$$(\rho C)_m = \frac{K_m}{\alpha_m} \quad .$$

8 The matching position also gives a particular value of η. Since

$$\eta = \frac{r}{2b_m}\sqrt{\frac{K_r(\rho C)_r}{K_m(\rho C)_m}} \quad ,$$

the value of $(\rho C)_r$ can be determined because K_r, K_m, and $(\rho C)_m$ have previously been determined.

Sample Calculations

The field data used in the following example are hypothetical, and were developed to illustrate the use of the graphical technique. A well penetrating a confined aquifer is injected with hot water at a uniform rate of 90.8 m^3/hr. The aquifer thickness, b_m is 40 m and the caprock thickness, b_r, is 20 m. Before the hot water with a uniform temperature of 70°C is injected, the aquifer and the caprock are at a uniform initial temperature of 20°C. At steady state, the aquifer temperature during the injection period is observed in five observation wells located at 10 m, 40 m, 60 m, 80 m and 100 m from the injection well. The resulting values of T_m in the five observation wells are listed in Table 1. Values of $r^2/b_r b_m$ and T are computed and appear in the righthand columns of Table 1.

Soon after injection started, temperatures were observed in the five observation wells. For this example, the data from the observation well 40 m from the injection well are used. Observations of t and T_m are listed in Table 2. Values of r^2/t and T are computed and shown in the righthand columns of Table 2.

First, values of K_m and K_r must be determined. To do this, values of T and $r^2/b_r b_m$ (from Table 1) are plotted on logarithmic paper. Type curves for the steady state solution are constructed on another sheet of logarithmic paper. The two sheets are superimposed and shifted (maintaining the coordinate axes parallel) until the field data points coincide with one of the type curves, as shown in Figure 8. At this matching position, the type curve gives $\omega = 90$. The

TABLE 1. TEMPERATURES MEASURED AT STEADY STATE CONDITION

r(m)	T_m(°C)	$r^2/b_r b_m$	T
10	70	0.125	1.000
40	69.35	2.00	0.987
60	68.65	4.50	0.973
80	67.60	8.00	0.952
100	66.30	12.50	0.926

TABLE 2. TEMPERATURES MEASURED AT UNSTEADY STATE CONDITION (r = 40 m).

t(hr)	T_m(°C)	r^2/t	T
0	20.0	-	0.000
1400	27.8	1.143	0.156
1600	46.8	1.000	0.544
1650	51.5	0.970	0.630
1700	55.05	0.941	0.701
1750	57.85	0.914	0.757
1800	60.00	0.889	0.800
1850	61.55	0.865	0.831
1900	62.70	0.842	0.854
1950	63.50	0.821	0.870
2000	64.10	0.800	0.883
2100	64.95	0.762	0.899

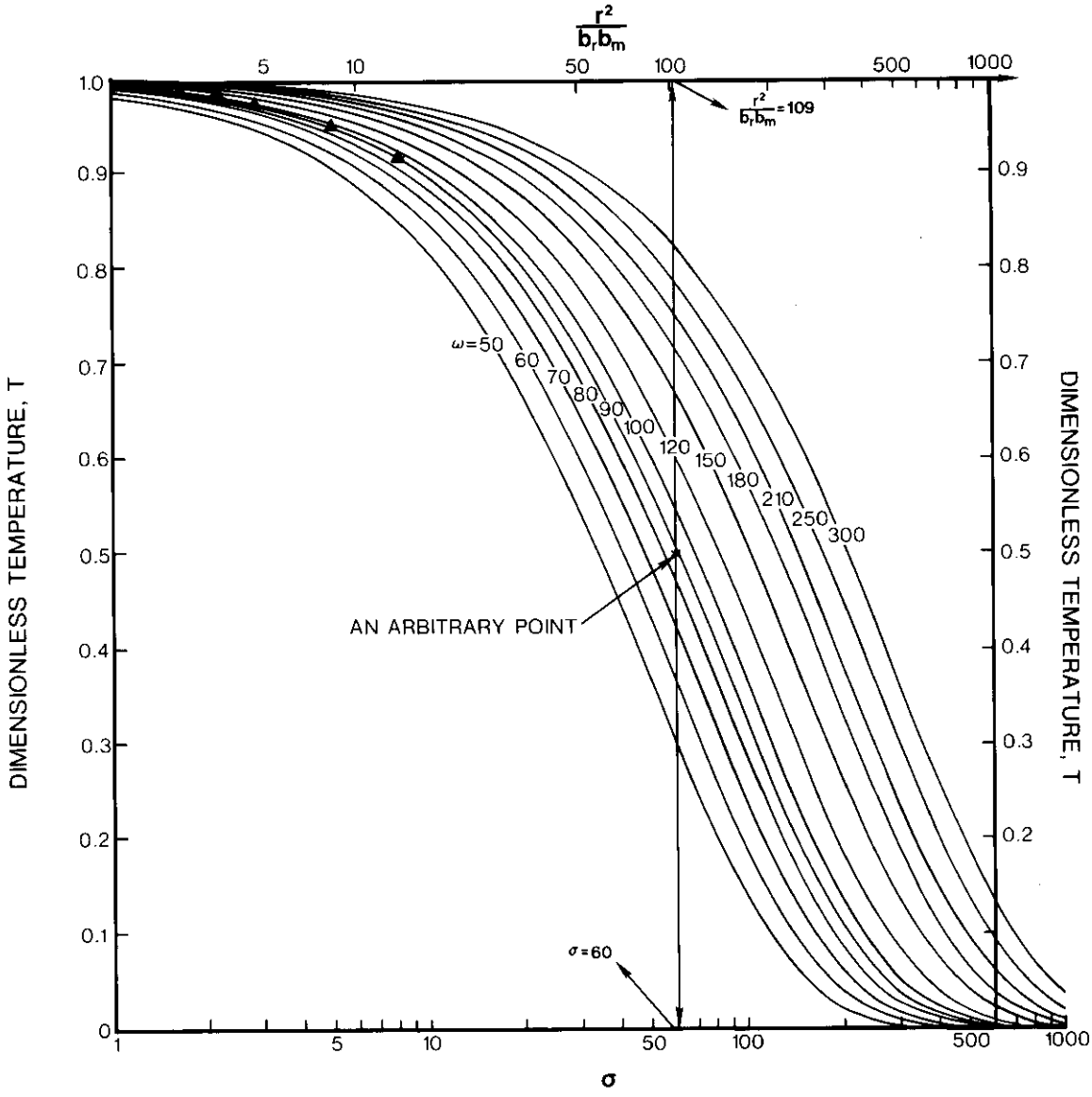

FIG. 8 Curve matching steady state type curve with field data to evaluate values of K_m and K_r.

value of K_m is determined from

$$\omega = \frac{(\rho C)_f Q}{4\pi b_m K_m} \quad ,$$

where $(\rho C)_f$ is usually considered constant and has the value of 4.187×10^6 $(J/m^3{}^\circ C)$. Thus,

$$K_m = \frac{(\rho C)_f Q}{4\pi b_m \omega} = \frac{(4.187 \times 10^6)(90.8)}{4\pi(40)(90)} = 8.404 \times 10^3 \left(\frac{\omega}{m^\circ C}\right) \quad .$$

A point selected at the matching position gives $r^2/b_m b_r = 109$ and $\sigma = 60$. The value of K_r is determined from

$$\sigma = \frac{r^2}{2b_m b_r} \frac{K_r}{K_m} \quad ,$$

or

$$K_r = 2\sigma K_m \left(\frac{r^2}{b_m b_r}\right)^{-1} = 2(60)(8.404 \times 10^3)(109)^{-1} =$$

$$9.252 \times 10^3 \left(\frac{\omega}{m^\circ C}\right) \quad .$$

After values of K_m and K_r are determined, values of $(\rho C)_m$ and $(\rho C)_r$ can be determined using the early time data. Values of T and r^2/t from Table 2 are plotted on logarithmic paper. Type curves for the short time period solution are constructed on another sheet of

logarithmic paper, using $\omega = 90$ (from steady state condition). The two sheets are superimposed and shifted, with coordinate axes parallel, until the observed data points concide with one of the type curves, as shown in Figure 9. From this matching position, the type curve gives $\eta = 0.5$, and $u = 90$; and from the field data curve $r^2/t = 1.0$, The value of α_m is determined from

$$u = \frac{r^2}{4\alpha_m t} \quad ,$$

or

$$\alpha_m = \frac{1}{4u}\frac{r^2}{t} = (\frac{1}{4})(\frac{1}{90})(1) = 2.778 \times 10^{-3}(\frac{m^2}{hr}) \quad .$$

Hence,

$$(\rho C)_m = \frac{K_m}{\alpha_m} = \frac{8.404 \times 10^3}{2.778 \times 10^{-3}} = 3.025 \times 10^6(\frac{J}{m^3 C}) \quad .$$

The value of $(\rho C)_r$ is determined from

$$\eta = \frac{r}{2b_m}[\frac{K_r}{K_m}\frac{(\rho C)_r}{(\rho C)_m}]^{1/2} \quad ,$$

where the value of r is the distance of the observation well from the injection well. In this example, r=40 m. Hence

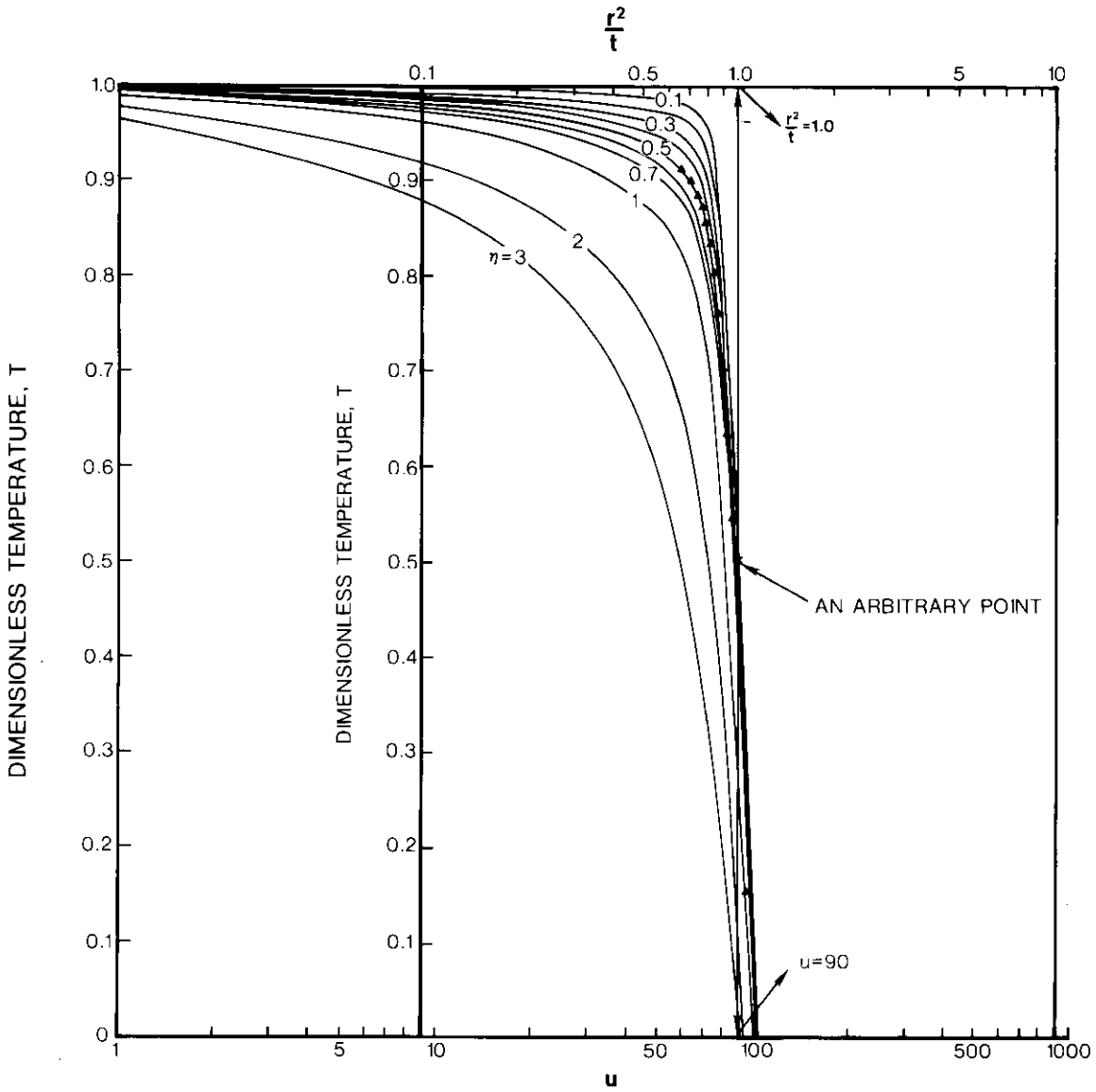

FIG. 9 Curve matching short time period type curve with field data to evaluate $(\rho C)_m$ and $(\rho C)_r$.

$$(\rho C)_r = 4\eta^2 \frac{b_m^2 K_m}{r^2 K_r}(\rho C)_m = 4(0.5)^2(\frac{40}{40})^2(\frac{8.404 \times 10^3}{9.252 \times 10^3})(3.025 \times 10^6) =$$

$$2.748 \times 10^6(\frac{J}{m^3 °C}) .$$

Therefore,

$$\alpha_r = \frac{K_r}{(\rho C)_r} = \frac{9.252 \times 10^3}{2.748 \times 10^6} = 3.367 \times 10^{-3}(\frac{m^2}{hr}) .$$

Discussion

In the mathematical sense, four unknowns can be uniquely determined by four distinct equations. Also, different curves represent different equations. So, two curves constructed from steady state and unsteady state field data represent two distinct equations. In addition, two curves constructed from the steady state and unsteady state solutions also represent two distinct equations. In the developed graphical method, the two field data curves are matched to the respective solution type curves. This means the equations are equated, so that the involved unknowns can be uniquely determined.

In the graphical sense, curves with no more than two parameters are representable in two-dimensional space. For example, Equation 85 has three parameters and is represented in Figures 2 and 3 with two

parameters, while one of the three parameters is kept constant, i.e. $\eta = 0.5$ in Figure 2 and $\omega = 90$ in Figure 3. Therefore, the use of only the unsteady state solution curves and data curves will not assure unique results.

The steady state solution has only two parameters, ω and σ. This means that the steady state solution must inevitably be used to determine the four pertinent thermal properties. Indeed, making use of the steady state solution and field data reduces the number of unknown thermal properties form four to two. It also supplies a value of ω which reduces the number of unknown parameters in the solution for short time periods from three to two. Consequently, the solution for short time periods can then be used to determine the remaining two thermal properties, $(\rho C)_m$ and $(\rho C)_r$.

After values of K_m and K_r are determined from the steady state condition, the number of unknown parameters in the solution for long time periods is also reduced to two, namely, δ and u. However, δ and u form the lower limit of integration in the solution, $(1+\delta)u$, which involves the remaining two undertermined thermal properties, $(\rho C)_m$ and $(\rho C)_r$. In addition, $(\rho C)_m$ and $(\rho C)_r$ do not appear in any other parameters in this solution. This makes it difficult to develop a graphical method using the long time period solution.

The preceeding discussion clearly explains the reason why the steady state solution and short time period solution are adopted for use in the present graphical method. In reality, however, obtaining field data approaching steady state conditions will be difficult

because of the extremely long times required to reach a steady state condition. For example in the sample calculation, the steady state condition would not be approached until the time after the injection started was longer than

$$\frac{b_r^2}{\alpha_r} = \frac{(20)^2}{3.367 \times 10^{-3}} = 1.188 \times 10^5 (hr) \quad .$$

This long period of time is mainly caused by the very low value of α_r. However, if the caprock thickness is small, the steady state condition can be approached within a reasonable period of time after injection starts. For instance, if b_r is only 4 m while all other conditions are the same as in the example calculation, then

$$\frac{b_r^2}{\alpha_r} = 198.0 (days) \quad ,$$

which might be achieved in practice. Therefore, the proposed graphical method for determining thermal properties, from an application standpoint, is more useful under conditions where the caprock thickness is small. For the condition where the caprock thickness is not small, an approximate method for graphically determining the thermal properties is developed and presented in the next section.

Before a value of α_r is determined, no information is available for evaluating the limit of the short time period solution. Data collected immediately after injection starts is presumed to satisfy

the short time period criterion. When the value of α_r is determined, the short time period creterion, $t \leq 0.1\ b_r^2/\alpha_r$, can be calculated, and the validity of $(\rho C)_m$ and $(\rho C)_r$ verified.

In this example, the time limit for using the short time period solution is about 1.188×10^4(hr), or 495 days. Obviously all the field data used were for times less than 495 days. Thus, the short time period solution is valid for these data. This large upper limit for the short time period reveals that if the caprock thickness is only moderately large (b_r > 10m), the solution for short time periods becomes the dominant equation in the problem. In other words, the aquifer temperature distribution is given by Equation 85 for most practical situations, if b_r > 10m and α_r is of the order of 0.003 to 0.004 m^2/hr.

Approximate Graphical Method

For most practical cases, K_r and K_m are about the same order of magnitude and $(\rho C)_r$ and $(\rho C)_m$ are also approximately the same order of magnitude. So, the assumption that $K/\alpha = 1.0$ appears reasonable. Thus, the definition of η is simplified to

$$\eta = \frac{r}{2b_m} \quad .$$

Since the value of r is the distance of the observation well from the

injection well, η is no longer an unknown. Under this condition, the solution for short time periods involves only two unknown parameters, ω and u. One pertinent thermal property, K_m, is involved in ω and the other pertinent thermal property, $(\rho C)_m$ is in u. Therefore, the short time period solution can be independently used to approximate K_m and $(\rho C)_m$. The procedure for this approximate graphical method is as follows:

1 Type curves for short time periods are constructed such that T versus the logarithm of u. Each curve corresponds to a particular value of ω. The parameter η is determined by the equation

$$\eta = \frac{r}{2b_m} \quad ,$$

where the values of r and b_m are known.

2 A data curve from the observation well in procedure 1 is constructed such that T versus the logarithm of r^2/t. The value of r should be the same one used to determine η.

3 Superimpose the data curve onto the type curves for short time periods, keeping the coordinate axes parallel and the logarithmic axes the same, until a matching position is obtained between the data curve and one of the type curves.

4 At the matching position, the value of ω for the matched type curve can be determined. Sometimes values of ω must be interpolated between two type curves. At the matching

position, a specific value of r^2/t and its associated value of u are obtained. Then K_m is determined from

$$K_m = \frac{(\rho C)_f Q}{4\pi b_m \omega} \quad .$$

α_m and $(\rho C)_m$ are determined from

$$\alpha_m = \frac{r^2}{4ut} \quad \text{and} \quad (\rho C)_m = \frac{K_m}{\alpha_m} \quad .$$

An example of this method is given by using the data from the previous example problem. Since r = 40 m and b_m = 40 m, η is equal to 0.5. The type curves for short time periods are constructed using η = 0.5. The field data points (T vs. log r^2/t) are plotted on another curve. The two curves are superimposed and shifted, keeping the coordinates axes parallel, until the data points coincide with one of the type curves, as shown in Figure 10. At this matching position, ω equals 90, and a match point gives r^2/t = 0.4 and u = 36.3. So, K_m is calculated as 8.404×10^3 (W/m°C) and $(\rho C)_m$ as 3.05×10^6 (J/m^3°C).

It is interesting that the value of K_m determined in this manner is identical with the value obtained by the more precise preceeding method, and the values of $(\rho C)_m$ differ by only 0.1 percent. This good approximation was caused by the fact that K/α = 0.976 in the original calculations ($K_m = 8.262 \times 10^3$ W/m°C, $K_r = 9.209 \times 10^3$ W/m°C,

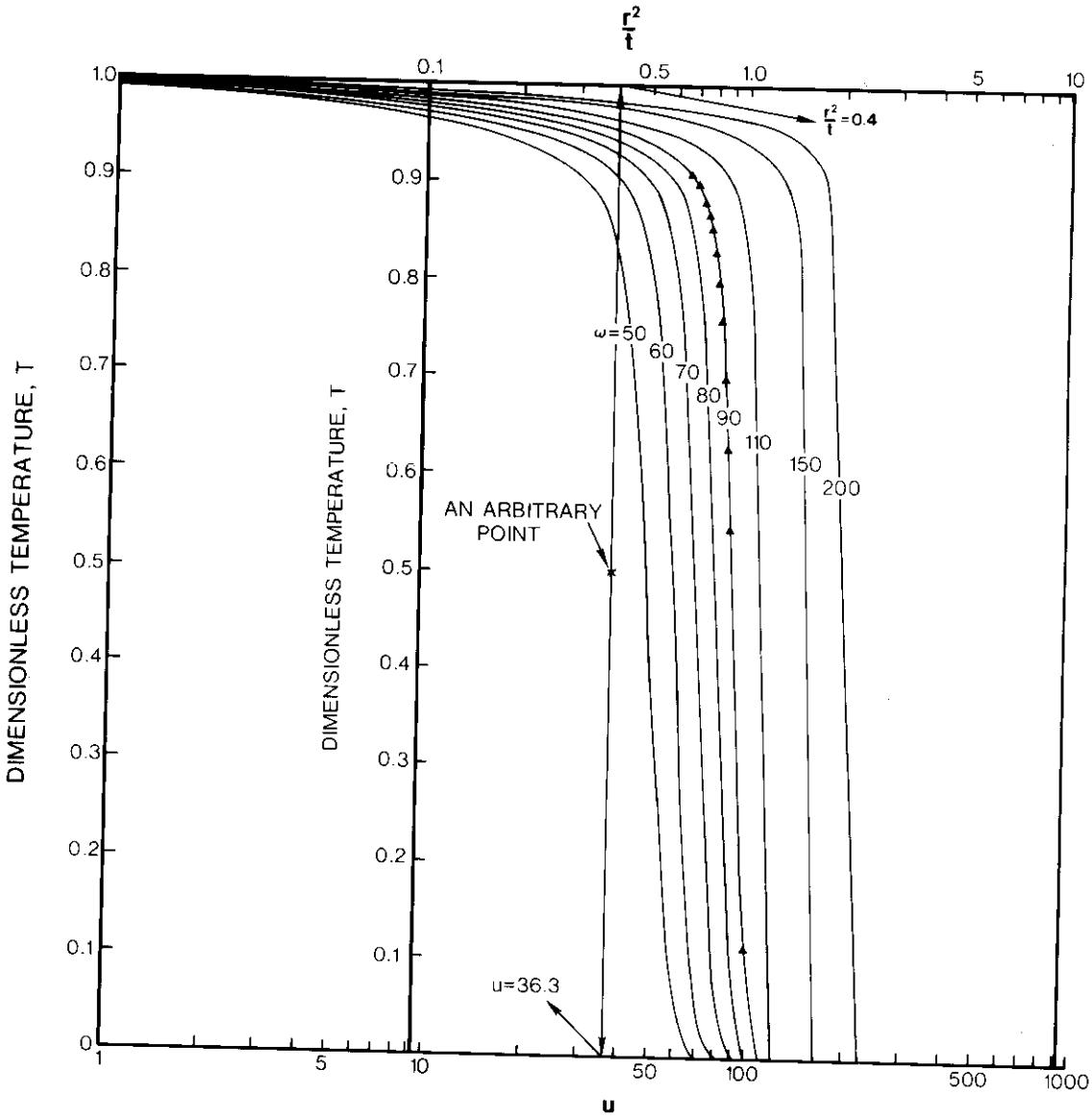

FIG. 10 Curve matching short time period type curve with field data to evaluate K_m and $(\rho C)_m$.

$(\rho C)_m$ = 2.851 x 10^6 J/m^3°C and $(\rho C)_r$ = 2.435 x 10^6 J/m^3°C). So, the assumption that $K/\alpha = 1.0$ in the approximate method should give good results for this problem.

To test the influence of the assumption that $K/\alpha = 1.0$ on the real condition that $K/\alpha \neq 1.0$, four figures, Figures 11, 12, 13 and 14, were prepared. In each figure, curves for the short time period solution are plotted for different values of the ratio, K/α. It was found that when $0.9 < K/\alpha < 1.1$, the assumption that $K/\alpha = 1.0$ yields reasonable results. The error caused by this assumption was less than 5 percent.

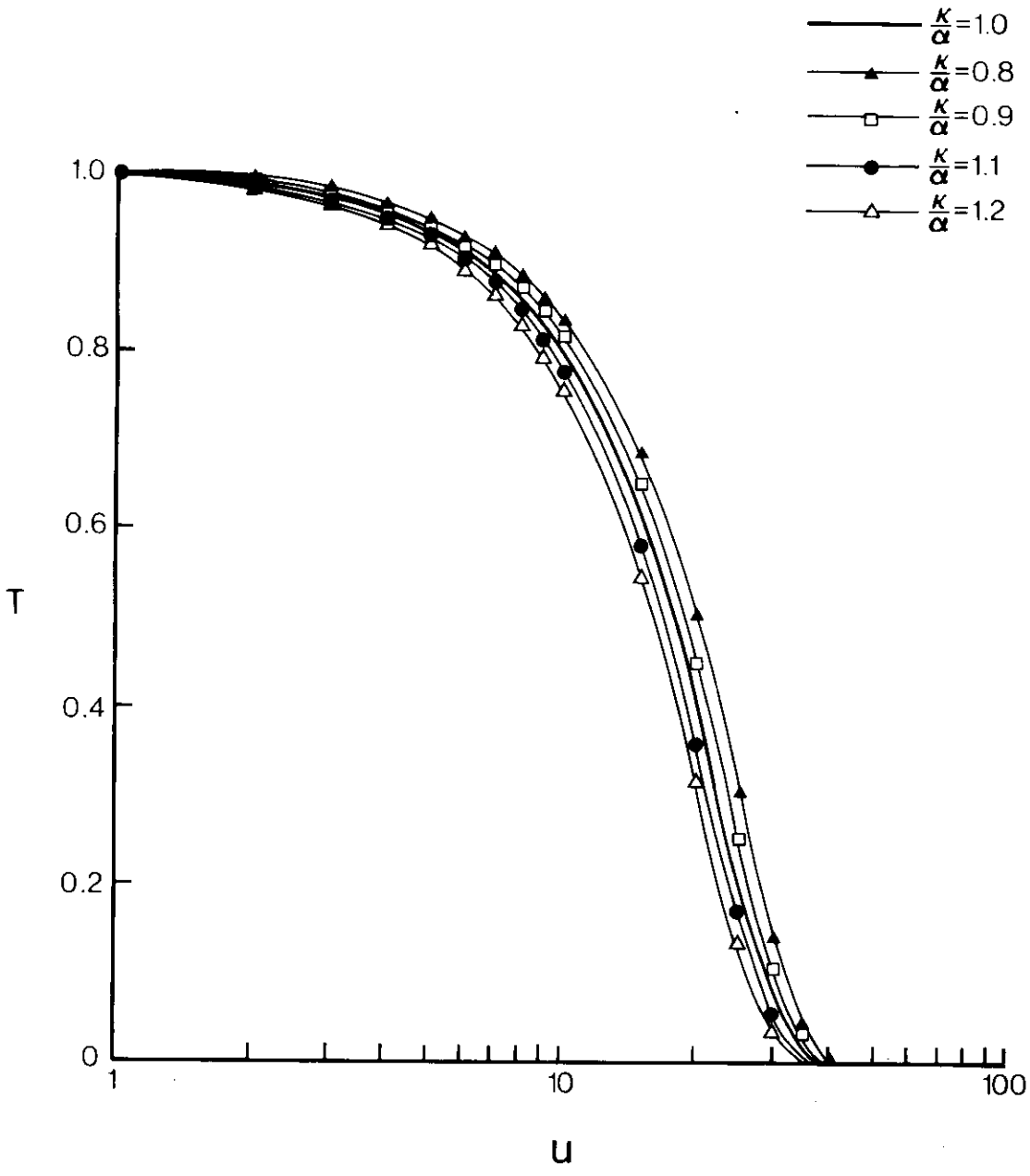

FIG. 11 Influence of + 10 percent variation in K/α on short time period solution (ω=50).

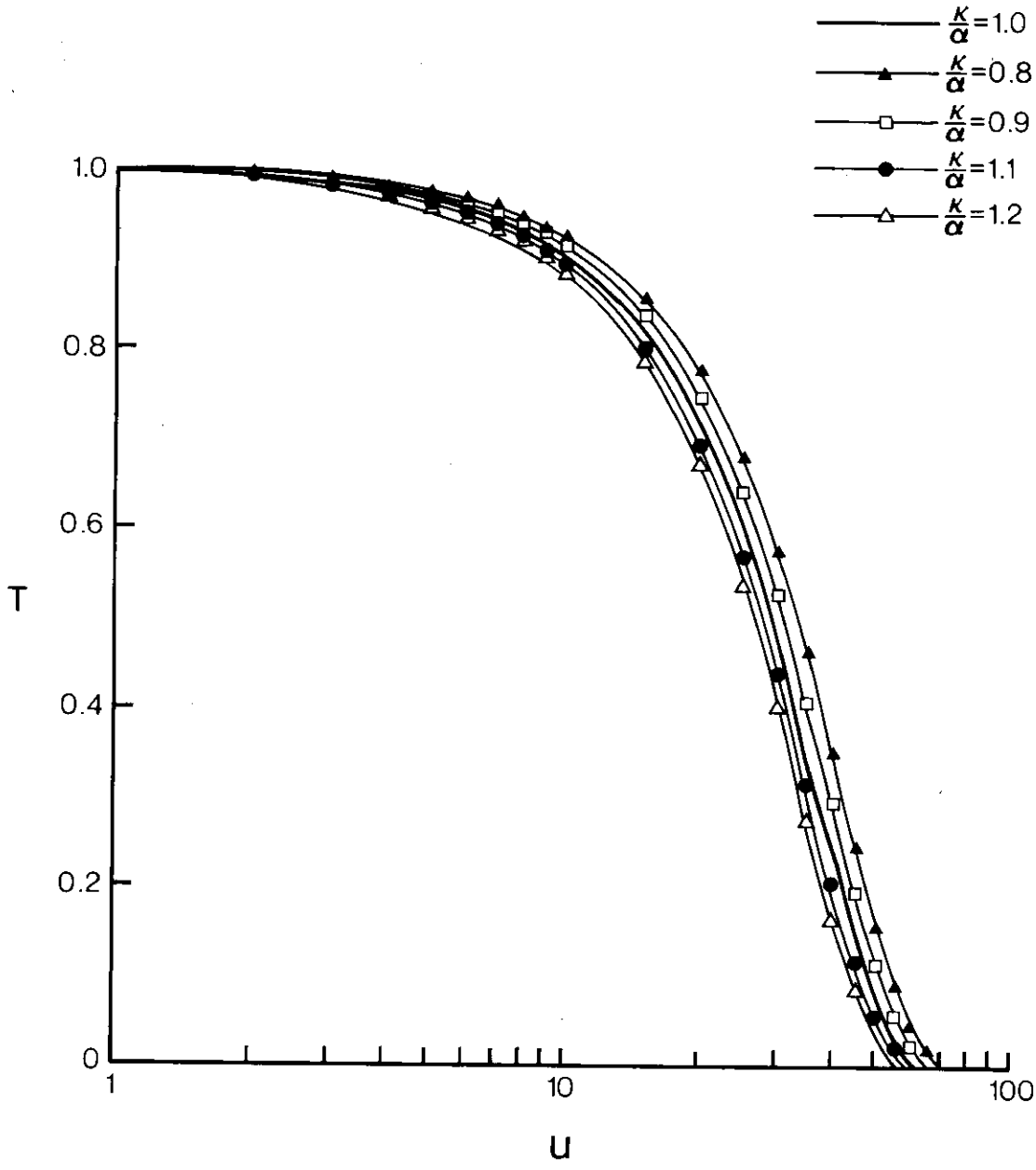

FIG. 12 Influence of + 10 percent variation in K/α on short time period solution (ω=100).

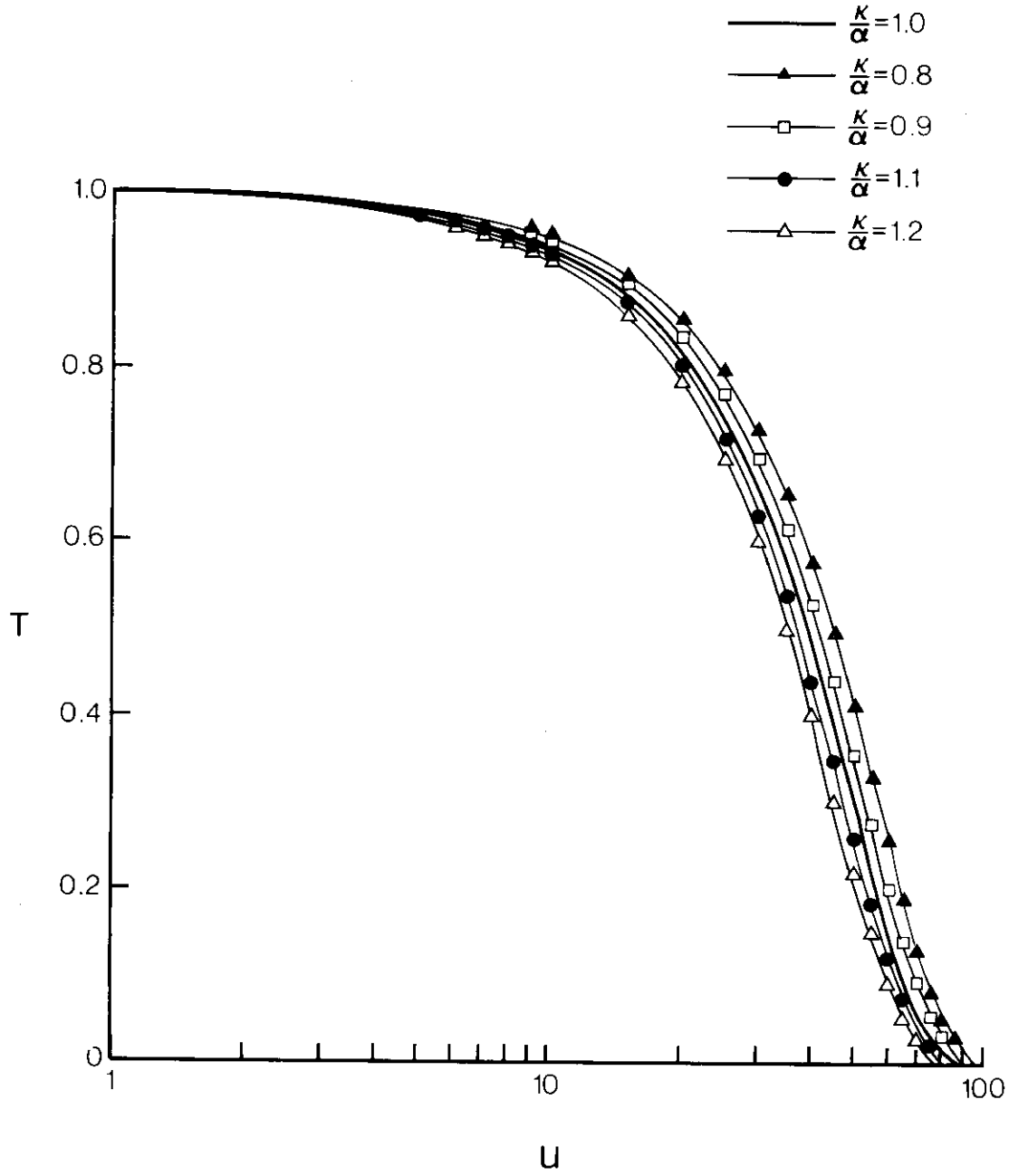

FIG. 13 Influence of + 10 percent variation in K/α on short time period solution ($\overline{\omega}$=150).

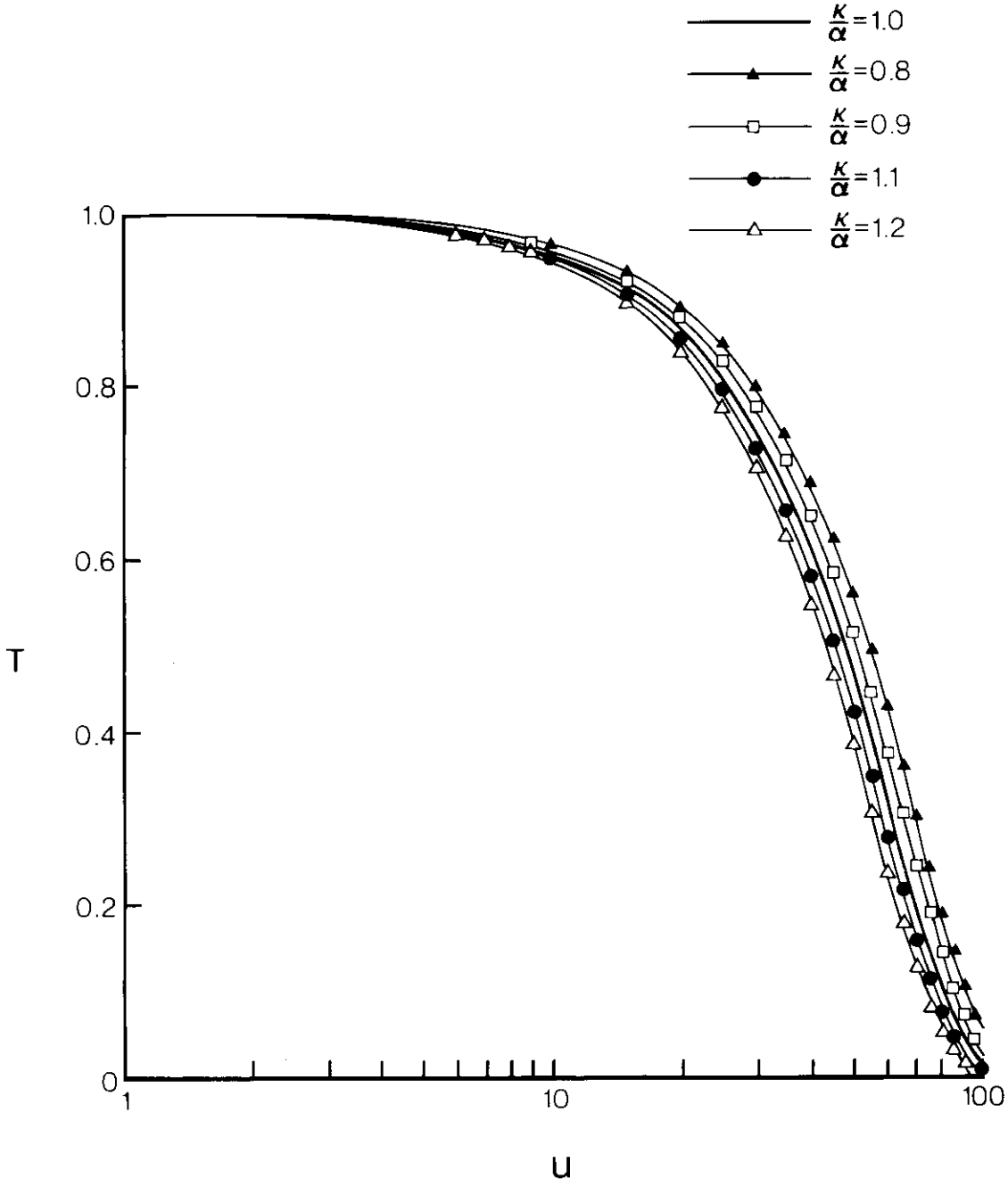

FIG. 14 Influence of + 10 percent variation in K/α on short time period solution (ω=200).

CHAPTER VII

SUMMARY, CONCLUSIONS AND RECOMMENDATIONS

Summary

In this study, two mathematical models, Model I and Model II, were developed to examine the influence of a finitely thick caprock on the thermal response in the aquifer during the thermal injection process. For both models, the caprock thickness was assumed finite.

Model I assumes that the vertical temperature distribution in the caprock is linear, and has a unsteady state and a steady state solution. The unsteady state solution for Model I is

$$T = \frac{1}{\Gamma(\omega)}\int_{u}^{\infty} e^{-x-\sigma/x} x^{\omega-1} dx \quad .$$

The steady state solution for Model I is

$$T = \frac{1}{\Gamma(\omega)}\int_{0}^{\infty} e^{-x-\sigma/x} x^{\omega-1} dx \quad .$$

Model II assumes that the vertical temperature distribution in the caprock is non-linear and two asymptotic solutions for the unsteady state case and an exact solution for the steady state case were obtained. One of the two asymptotic solutions is for short time

periods, $t \leq 0.1\ b_r^2/\alpha_r$, and is expressed as

$$T = \frac{1}{\Gamma(\omega)}\int_u^{\infty} e^{-x}\mathrm{Erfc}\left[\frac{\eta\sqrt{u}}{\sqrt{x(x-u)}}\right] x^{\omega-1}dx \quad .$$

The other asymptotic solution is for long time periods, $t \geq b_r^2/\alpha_r$, and is expressed as

$$T = \frac{1}{\Gamma(\omega)}\int_{(1+\delta)u}^{\infty} e^{-x-\sigma/x}x^{\omega-1}dx \quad .$$

The steady state solution for Model II is identical with that for Model I.

Using the unsteady state solution for short time periods and the steady state solution in Model II, a graphical technique was developed for determining four pertinent aquifer thermal properties: (1) the horizontal thermal conductivity of the aquifer, K_m, (2) the thermal capacity of the aquifer, $(\rho C)_m$, (3) the vertical thermal conductivity of the caprock, K_r, and (4) the thermal capacity of the caprock, $(\rho C)_r$. Dimensionless type curves are constructed from the steady state solution and from the unsteady state solution for short time periods. Using field data, one field curve is constructed using long-term temperature observations (approaching steady state) from several observation wells, and a second curve is constructed using short-time temperature observations from any one of the observation wells. These curves are then matched with the appropriate dimension-

less type curves, and values of the four aquifer thermal properties evaluated.

Since it is difficult to attain the steady state condition in the field, an approximate graphical technique for evaluating the parameters is developed without using the steady state field data. In this approximate method, K_r is assumed equal to K_m, and $(\rho C)_r$ is assumed equal to $(\rho C)_m$.

Conclusions

This study permitted the following conclusions to be drawn:

1 The caprock thickness influences the temperature distribution in the aquifer only when the time after injection is long.

2 Schapery's approximate method for inverting Laplace transforms yielded satisfactory results to this problem only after large times.

3 An exact solution for the temperature distribution in an aquifer was obtained for steady state conditions. Two asymptotic solutions for the temperature distribution in an aquifer were obtained under unsteady state conditions; one is for short time periods, and the other is for long time periods. No solution was obtained for the intermediate time interval.

4 The short time period unsteady solution will suffice for analyzing most practical problems.

5 A graphical method was developed to evaluate four thermal properties: (1) the horizontal thermal conductivity in the

5 (Continued) aquifer, (2) the thermal capacity in the aquifer, (3) the vertical thermal conductivity in the caprock, and (4) the thermal capacity in the caprock. This graphical method uses field measurements of aquifer temperatures and type curves prepared from the analytical solution.

6 A modified graphical method was developed to evaluate the horizontal thermal conductivity and the thermal capacity in the aquifer. In this modified method, the vertical thermal conductivity in the caprock is assumed to be equal to the horizontal thermal conductivity in the aquifer, and the thermal capacity in the caprock is assumed to be equal to that in the aquifer.

Recommendations

This study showed the following areas to be in particular need of additional work:

1 Comparison of the analytical solutions with field data.

2 The exact Laplace inversion of Equation 82 needs to be found.

REFERENCES

1 Abramowitz, M. and I. A. Stegun. 1970. Handbook of Mathematical Functions. Dover Publications, Inc., New York.

2 Avdonin, N. A. 1964. Some Formulas for Calculating the Temperature Field of a Stratum Subjected to Thermal Injection. Neft'i Gaz 7(3):37-41.

3 Baker, P. E. 1967. Heat Wave Propagation and Heat Losses in Thermal Oil Recovery Processes. Proc., 7th World Pet. Congress, 3:459-470.

4 Bateman, H. 1953. Tables of Integral Transforms. Vol. II. McGraw-Hill Book Company, New York.

5 Carslaw H. S. and J. C. Jaeger. 1959. Conduction of Heat in Solids. Oxford University Press, London.

6. Chow, V. T. 1952. On the Determination of Transmissibility and Storage Coefficients from Pumping Test Data. Amer. Geophysical Union, Washington, D.C., 33:397-404.

7 Cooper, H. H., Jr. and C. E. Jacob. 1946. A generalized Graphical Method for Evaluating Formation Constants and Summarizing Well-Field History. Trans. Amer. Geophysical Union, Washington, D.C., 27:526-534.

8 Davison, R. R., W. B. Harris and J. H. Martin. 1975. Storing Sunlight Underground. Chemical Technology. 5:736-741.

9 Ditkin, V. A. and P. I. Kuznetsov. 1951. Handbook on Operator Calculations (In Russian). State Publishing House of Theoretical and Technical Literature, New York.

10 Henrici, P. 1977. Applied and Computational Complex Analysis. Vol. II. John Wiley and Sons, Inc., New York.

11 Jenkins, R. and J. S. Aronofsky. 1954. Analysis of Heat Transfer Processes in Porous Media - New Concepts in Reservoir Heat Engineering. Proc. 18th Tech. Conf. on Petr. Prod., Penn. State University (64):69-74.

12 Kriz, G. J., V. H. Scott and R. H. Burgy. 1966. Graphical Determination of Confined Aquifer Parameters. Proc. of the Amer. Soc. of Civil Eng., HY5:39-48.

13 Lauwerier, H. A. 1955. The Transport of Heat in an Oil Layer Caused by the Injection of Hot Fluid. Appl. Sci. Res., Sec. A. 5:145-150.

14 Olver F. W. J. 1974. Asymptotics and Special Functions. Academic Press, New York.

15 Roberts, G. E. and H. Kaufman. 1966. Table of Laplace Transforms. W. B. Saunders Co., Philadelphia and London.

16 Rubinshtein, L. I. 1959. The Total Heat Loss in Injection of a Hot Liquid into a Stratum. Neft'i Gaz 2(9):41-48.

17 Rubinshtein, L. I. 1960. A Contact Thermal Conduction Problem. Dan SSSR 135(4):805-808.

18 Rubinshtein, L. I. 1963. An Asymptotic Solution of an Axially Symmetric Contact Problem in Thermal Convection for Higher Values of the Convection Parameter. Dan SSSR 146(5):1043-1046.

19 Schapery, R. A. 1962. Approximate Methods of Transform Inversion for Viscoelastic Stress Analysis. Proc. 4th Congress. Appl. Mechs. 2:1075-1085.

20 Sneddon, I. H. 1972. The Use of Integral Transforms. McGraw-Hill Book Company, New York.

21 Spillette. A. G. 1965. Heat Transfer During Hot Fluid Injection into an Oil Reservoir. J. of Canadian Pet. Tech. 4(4):213-217.

22 Theis. C. V. 1935. The Relation Between the Lowering of the Piezometric Surface and the Rate and Duration of Discharge of a Well Using Groundwater Storage. Trans. Amer. Geophysical Union, Washington, D.C., 16:519-524.

23 Thomas, G. W. 1967. Approximate Methods for Calculating the Temperature Distribution During Hot Fluid Injection. J. of Canadian Pet. Tech. 6(4):123-129.

24 Watson, G. N. 1922. A Treatise on the Theory of Bessel Functions. Cambridge University Press, London.

25 Whittaker, E. T. and G. N. Watson. 1927. A Course of Modern Analysis. Cambridge University Press, London.

26 Wylie, C. R. 1960. Advanced Engineering Mathematics. McGraw-Hill Book Company, New York.

APPENDICES

APPENDIX A

DERIVATION OF THE HEAT EQUATION FOR THE AQUIFER

The general heat equation in the aquifer for both models can be derived by combining the principles of conservation of mass and energy, Darcy's law and Fourier's law. Because of the assumptions made, the result is a linear, second order partial differential equation which involves two dependent variables, time and radial distance. All the assumptions were given in Chapter IV and are not reproduced here.

The principle of conservation of energy when applied to a volume element of porous media fixed in space can be stated as:

(Rate of energy inflow) - (Rate of energy outflow) =

(Rate of change of energy inside the volume element) .

Applying this principle to the volume element shown in Figure A-1 results in

$$H_r - H_{r+dr} - H_c = \partial H_v / \partial t \quad , \quad \text{.....} \quad [A\text{-}1]$$

where

$$H_r = \left(-K_m \frac{\partial T_m}{\partial r} + (\rho C)_f V_f T_f\right) A_r \quad ,$$

is the rate of energy inflow across face A_r, T_f is the fluid flow temperature and V_f is the Darcy volume flux of flow;

$$H_{r+dr} = \left(-K_m \frac{\partial T_m}{\partial r} + (\rho C)_f V_f T_f\right) A_{r+dr} \quad ,$$

is the rate of energy outflow across face A_{r+dr} ;

$$H_c = -K_r \left.\frac{\partial T_r}{\partial z}\right|_{z=0} A_c \quad ,$$

is the rate of energy outflow across the top face of the aquifer A_c; and

$$H_v = (\rho C)_m V_m T_m \quad ,$$

is the energy contained inside the volume element V_m . Note that the chosen volume element is assumed to be symetrical about the midpoint of the aquifer.

Furthermore, H_r is assumed to include only heat conduction and convection in the aquifer. The term $-K_m \partial T_m / \partial r$ is the expression for heat conduction, and the term $(\rho C)_f V_f T_f$ is the expression for heat convection. By assuming that the temperature of the sand in the aquifer and its surrounding fluid reach thermal equilibrium instantaneously, $T_f = T_m$. Applying a Taylor series expansion about H_r and neglecting the second and higher order terms,

$$H_r - H_{r+dr} = -\frac{\partial H_r}{\partial r} dr \quad . \quad \text{.....} \quad [A\text{-}2]$$

Substituting

$$H_r = (-K_m \frac{\partial T_m}{\partial r} + (\rho C)_f V_f T_m) A_r$$

into Equation A-2 and performing the necessary differentions results in

$$H_r - H_{r+dr} =$$

$$\pi r b_m [K_m \frac{\partial T^2_m}{\partial r^2} + (\frac{K_m}{r} - (\rho C)_f V_f) \frac{\partial T_m}{\partial r} - (\rho C)_f T_m (V_f + r \frac{dV_f}{dr})] dr \quad . \quad [A-3]$$

Since the fluid flux V_f is steady, and the injection rate Q is constant,

$$V_f = \frac{Q}{2\pi b_m r} \quad ,$$

or

$$r \frac{dV_f}{dr} = r(-\frac{Q}{2\pi b_m r}) = -V_f \quad .$$

From the above equation, it is found that

$$V_f + r \frac{dV_f}{dr} = 0 \quad ,$$

and Equation A-3 is simplified to

$$H_r - H_{r+dr} = \pi r b_m [K_m \frac{\partial^2 T_m}{\partial r^2} + (\frac{K_m}{r} - \frac{(\rho C)_f Q}{2\pi b_m r}) \frac{\partial T_m}{\partial r}] \, dr \quad . \quad .. \quad [A-4]$$

The term H_c in Equation A-1 is the heat loss from the top surface of the aquifer into the caprock. Expressing A_c in its differential form, H_c can be written as

$$H_c = -\pi r b_m \left(2\frac{K_r}{b_m}\frac{\partial T_r}{\partial z}\bigg|_{z=0}\right) dr \quad . \quad \text{.....} \quad [A\text{-}5]$$

The term $\partial H_v/\partial t$ on the right hand side of Equation A-1 is expressed in differential form as

$$\frac{\partial H_v}{\partial t} = (\rho C)_m \, r b_m \frac{\partial T_m}{\partial t} dr \quad . \quad \text{.....} \quad [A\text{-}6]$$

Placing Equations A-4, A-5 and A-6 into Equation A-1, and cancelling the common term $(\pi r b_m dr)$, the heat equation in the aquifer becomes

$$K_m \frac{\partial^2 T_m}{\partial r^2} + \left(K_m - \frac{(\rho C)_f Q}{2\pi b_m}\right)\frac{1}{r}\frac{\partial T_m}{\partial r} + 2\frac{K_r}{b_m}\frac{\partial T_r}{\partial z}\bigg|_{z=0} = (\rho C)_m \frac{\partial T_m}{\partial t} \quad .$$

Dividing the above equation by K_m, and letting $\omega = \dfrac{(\rho C)_f Q}{4\pi b_m K_m}$ and $\alpha_m = \dfrac{K_m}{(\rho C)_m}$, the heat equation in the aquifer becomes

$$\frac{\partial^2 T_m}{\partial r^2} + \frac{(1-2\omega)}{r}\frac{\partial T_m}{\partial r} + 2\frac{K_r}{K_m b_m}\frac{\partial T_r}{\partial z}\bigg|_{z=0} = \frac{1}{\alpha_m}\frac{\partial T_m}{\partial t} \quad . \quad \text{.....} \quad [A\text{-}6]$$

Equation A-6 is the same one given as Equation 33 in the text.

APPENDIX B

DERIVATION OF SOLUTIONS FOR MODEL I AND MODEL II

The problem to be solved was posed in Chapter V by Equation 60, 61 and 62. They are reproduced here,

$$\frac{d^2U}{dR^2} + \frac{1 - 2\omega}{R}\frac{dU}{dR} - \xi U = pU \quad , \qquad \text{[B-1]}$$

$$U(0, p) = 1/p \quad , \qquad \text{[B-2]}$$

$$U(\infty, p) = 0 \quad . \qquad \text{[B-3]}$$

Comparing Equation B-1 with the differential equation in Theorem 1 and letting

$a = 1 - 2\omega$, $e = 0$, $g = 0$, $d = -(\xi + p)$, $q = 1$ and $f \neq 0$, then

$$\mu = \frac{1 - (1-2\omega)}{2} = \omega \quad ,$$

$$\beta = 0 \quad ,$$

$$\lambda = \sqrt{\xi+p} \quad ,$$

$$\nu = \omega \quad ,$$

and all other restrictions stated in Theorm 1 are satisfied. The complete solution for Equation B-1, is

$$U = R^{\omega}[C_1 I\omega(R\sqrt{\xi+p}) + C_2 K\omega(R\sqrt{\xi+p})] \quad , \qquad \text{[B-4]}$$

where C_1 and C_2 are two constants to be determined from the boundary conditions.

As R approaches infinity, I $(R\sqrt{\xi+p})$ approaches infinity while $K_\omega(R\sqrt{\xi+p})$ is bounded. Therefore, the boundary condition at $R = \infty$, Equation B-3, forces C_1 to be zero.

The constant C_2 is determined using the other boundary condition, Equation B-2. From Equation 16, it is found that

$$C_2 = \frac{2^{1-\omega}(\xi+p)^{\omega/2}}{\Gamma(\omega)p} \quad .$$

Placing these values for C_1 and C_2 into the above equation, Equation B-4, results in

$$U = \frac{2^{1-\omega}R^\omega}{\Gamma(\omega)} \frac{(\xi+p)^{\omega/2}K_\omega(R\sqrt{\xi+p})}{p} \quad ,$$

or

$$T = \frac{2^{1-\omega}R^\omega}{\Gamma(\omega)} L^{-1}\{\frac{(\xi+p)^{\omega/2}K_\omega(R\sqrt{\xi+p})}{p}\} \quad . \quad \text{.....} \quad [B\text{-}5]$$

The inversion of Equation B-5 is determined as follows. From Equation 24,

$$L^{-1}\{p^{\omega/2}K_\omega(R\sqrt{p})\} = \frac{R^\omega}{(2\tau)^{1+\omega}} \exp\{\frac{-R^2}{4\tau}\} \quad . \quad \text{.....} \quad [B\text{-}6]$$

Applying the translation law, given in Equation 22, to Equation B-6

results in

$$L^{-1}\{(p+\xi)^{\omega/2}\ K\omega(R\sqrt{p+\xi})\}= \frac{R^{\omega}}{(2\tau)^{1+\omega}} \exp\{\frac{-R^2}{4\tau} - \xi\tau\} \quad . \quad \ldots \quad [B\text{-}7]$$

Applying the convolution law, given in Equation 23, to Equation B-7, results in

$$L^{-1}\{\frac{(p+\xi)^{\omega/2}K_{\omega}(R\sqrt{p+\xi})}{p}\}= \int_0^{\tau} \frac{R^{\omega}}{(2x)^{1+\omega}} \exp\{\frac{-R^2}{4x} - \xi x\}dx \quad . \quad .. \quad [B\text{-}8]$$

Placing Equation B-8 into Equation B-5 results in

$$T = \frac{1}{\Gamma(\omega)}(\frac{R^2}{4})^{\omega}\int_0^{\tau} \exp\{\frac{-R^2}{4x} - \xi x\}\frac{dx}{x^{1+\omega}} \quad .$$

Making a change of variable, $y = R^2/4x$, in the above equation results in

$$T = \frac{1}{\Gamma(\omega)}\int_u^{\infty} \exp(-y - \frac{\sigma}{y})y^{\omega-1}\ dy \quad , \quad \ldots\ldots\ldots\ldots\ldots\ldots \quad [B\text{-}9]$$

where $u = R^2/4\tau = r^2/4\alpha_m t$, and $\sigma = \xi R^2/4 = r^2/2b_m b_r(K_r/K_m)$.

In Model II, the solution for long time periods in terms of Laplace transforms was given in Equation 87,

$$U = \frac{2^{1-\omega}R^{\omega}}{\Gamma(\omega)} \frac{(\delta' p+\xi)^{\omega/2}K\ (R\sqrt{\delta' p+\xi})}{p} \quad ,$$

or

$$T = \frac{2^{1-\omega}R^{\omega}}{\Gamma(\omega)} L^{-1}\{\frac{(\delta' p+\xi)^{\omega/2} K\omega(R\sqrt{\delta' p+\xi})}{p}\} \quad . \quad \ldots\ldots\ldots\ldots \quad [B\text{-}10]$$

The inversion of Equation B-10 can be written using the following identity,

$$L^{-1}\{\frac{(\delta' p+\xi)^{\omega/2} K\omega(R\sqrt{\delta' p+\xi})}{p}\} = \delta' L^{-1}\{\frac{(\delta' p+\xi)^{\omega/2} K\omega(R\sqrt{\delta' p+\xi})}{\delta' p}\} \quad .$$

The inversion of the right hand side of the above equation is obtained using the change of scale law, Equation 21,

$$L^{-1}\{\frac{(\delta' p+\xi)^{\omega/2} K\omega(R\sqrt{\delta p+\xi})}{p}\} = \int_0^{\tau/\delta'} \frac{R^{\omega}}{(2x)^{1+\omega}} \exp\{\frac{-R^2}{4x} - \xi x\}dx \quad .$$

It is clear that Equation B-10 becomes

$$T = \frac{1}{\Gamma(\omega)} \int_{(1+\delta)u}^{\infty} \exp(-y - \frac{\sigma}{y})\, y^{\omega-1}\, dy \quad . \quad \ldots\ldots\ldots\ldots \quad [B\text{-}11]$$

Equation B-11 is the solution for long time periods in Model II.

APPENDIX C

USING THE LAPLACE-CARSON TRANSFORM TO SOLVE MODEL II.

The solution for short time periods in Model II is obtained using Laplace-Carson transforms. The mathematical equations for Model II are

$$\frac{\partial^2 T_1}{\partial Z^2} = \frac{1}{\alpha^2}\frac{\partial T_1}{\partial \tau} \quad , \qquad \text{..... [C-1]}$$

$$\frac{\partial^2 T}{\partial R^2} + \frac{1 - 2\omega}{R}\frac{\partial T}{\partial R} + K\frac{\partial T_1}{\partial Z}\bigg|_{Z=0} = \frac{\partial T}{\partial \tau} \quad , \qquad \text{..... [C-2]}$$

$$T_1(R, Z, 0) = 0 \quad , \qquad \text{..... [C-3]}$$

$$T_1(R, b, \tau) = 0 \quad , \qquad \text{..... [C-4]}$$

$$T_1(R, 0, \tau) = T(R, \tau) \quad , \qquad \text{..... [C-5]}$$

$$T(R, 0) = 0 \quad , \qquad \text{..... [C-6]}$$

$$T(0, \tau) = 1 \quad , \text{ and} \qquad \text{..... [C-7]}$$

$$T(\infty, \tau) = 0 \quad . \qquad \text{..... [C-8]}$$

The Laplace-Carson transform is applied to T_1 and T with respect to τ, then

$$U_1(R, Z, p) = Lc[T_1(R, E, \tau)]$$

and $U(R, Z, p) = Lc[T(R, Z, \tau)]$.

Thus, Equations C-1 to C-8 become

$$\frac{d^2U_1}{dZ^2} = \frac{p}{\alpha^2} U_1 \quad \text{..... [C-9]}$$

$$\frac{d^2U}{dR^2} + \frac{1 - 2\omega}{R} \frac{dU}{dR} + K\frac{dU_1}{dZ}\bigg|_{Z=0} = pU \quad \text{..... [C-10]}$$

$$U_1(R, b, p) = 0 \ , \quad \text{..... [C-11]}$$

$$U_1(R, 0, p) = U(R, p) \ , \quad \text{..... [C-12]}$$

$$U(0, p) = 1 \ , \quad \text{and} \quad \text{..... [C-13]}$$

$$U(\infty, p) = 0 \ . \quad \text{..... [C-14]}$$

The solution for Equations, C-9, C-11, and C-12 is

$$U_1 = U \frac{\sinh[(b-z/\alpha)\sqrt{p}]}{\sinh b/\alpha\sqrt{p}} \ .$$

So, $\frac{dU_1}{dZ}\bigg|_{Z=0} = U - \frac{\sqrt{p}}{\alpha} \coth(b/\alpha\sqrt{p})$.

Substituting the above equation Equation C-10 results in

$$\frac{d^2U}{dR^2} + \frac{1 - 2\omega}{R}\frac{dU}{dR} - [p + \frac{K}{\alpha}\sqrt{p}\ \coth(b/\alpha\sqrt{p})]U = 0 \quad .$$

The above equation is solved using Theorem 1, and the two boundary conditions, Equations C-13 and C-14. The result is

$$U = \frac{2^{1-\omega}R^{\omega}}{\Gamma(\omega)}\ [\chi^{\omega/2}K_{\omega}(R\sqrt{\chi})] \quad .$$

For short time periods, p is large. Thus, for $b^2p/\alpha^2 \geq 10$, χ is written as

$$\chi = p + K/\alpha\sqrt{p} \quad .$$

Thus

$$T = \frac{2^{1-\omega}R^{\omega}}{\Gamma(\omega)}\ Lc^{-1}[(p + K/\alpha\sqrt{p})^{\omega/2}K_{\omega}(R\sqrt{p+K/\alpha\sqrt{p}})] \quad . \quad \ldots\ldots \quad [C\text{-}15]$$

Let F(p) denote the function in the brackets of Equation C-15 and $m = K/\alpha$, then

$$F(m^2p) = m^{\omega}[(p+\sqrt{p})^{\omega/2}K_{\omega}(mR\sqrt{p+\sqrt{p}})] \quad . \quad \ldots\ldots\ldots\ldots\ldots \quad [C\text{-}16]$$

Equation C-16 is written in the identity as

$$F(m^2p) = m^{\omega}/p\ \frac{p}{p+\sqrt{p}}\ \{(p+\sqrt{p})^{\omega/2+1}K_{\omega}(mR\sqrt{p+\sqrt{p}})\} \quad \ldots\ldots\ldots \quad [C\text{-}17]$$

From Equation 30,

$$Lc^{-1}\{p^{\omega/2+1}K_\omega(mR\sqrt{p})\} = \frac{(mR)^\omega}{(2\tau)^{1+\omega}}\exp(-\frac{m^2R^2}{4\tau}) \quad \text{..... [C-18]}$$

From Equation 28,

$$Lc^{-1}\{\frac{p}{p+\sqrt{p}}(p+\sqrt{p})^{\omega/2+1}K_\omega(mR\sqrt{p+\sqrt{p}})\} =$$

$$(mR)^\omega\int_0^\tau \frac{x}{2\sqrt{\pi(\tau-x)^3}}\exp(\frac{-x^2}{4(\tau-x)} - \frac{m^2R^2}{4x})\frac{dx}{2x^{1+\omega}} \quad \text{..... [C-19]}$$

By the convolution law,

$$Lc^{-1}\{1/p\ \frac{p}{p+\sqrt{p}}(p+\sqrt{p})^{\omega/2+1}K_\omega(mR\sqrt{p+\sqrt{p}})\} =$$

$$(mR)^\omega\int_0^\tau ds\int_0^s \frac{x}{2\sqrt{\pi(s-x)^3}}\exp\{-\frac{x}{4(s-x)} - \frac{m^2R^2}{4x}\}\frac{dx}{(2x)^{1+\omega}} \quad \text{[C-20]}$$

Replacing the result obtained from Equation C-20 into Equation C-16 gives

$$Lc^{-1}\{F(m^2p)\} = (m^2R)^\omega\int_0^\tau ds\int_0^s \frac{x}{2\sqrt{\pi(s-x)^3}}\exp\{\frac{-x^2}{4(s-x)} - \frac{m^2R^2}{4x}\}\frac{dx}{(2x)^{1+\omega}}$$

Applying the change of scale law, given in Equation 29 to the above

equation results in

$$Lc^{-1}\{F(p)\} = (m^2R)^{\omega}\int_0^{m^2\tau} ds \int_0^{s} \frac{x}{2\sqrt{\pi}(s-x)^3} \exp\{\frac{-x^2}{4(s-x)} - \frac{m^2R^2}{4x}\}\frac{dx}{(2x)^{1+\omega}} \quad .$$

Substitutuing the above equation into Equation C-15 results in

$$T = \frac{1}{\Gamma(\omega)}(\frac{m^2R^2}{4})^{\omega}\int_0^{m^2\tau} ds \frac{1}{2\sqrt{\pi}} \int_0^{s} \frac{x}{(s-x)^{3/2}} \exp\{\frac{-x^2}{4(s-x)} - \frac{m^2R^2}{4x}\} \frac{dx}{x^{1+\omega}} \quad .$$

Making a change in the order of integration in the above equation results in

$$T = \frac{1}{\Gamma(\omega)}(\frac{m^2R^2}{4})^{\omega}\int_0^{m^2\tau} \exp\{\frac{-m^2R^2}{4x}\} \frac{dx}{x^{1+\omega}} \frac{1}{2\sqrt{\pi}} \int_x^{m^2\tau} \frac{\exp\{ - \frac{x^2}{4(s-x)}\} x \, ds}{(s-x)^{3/2}} \quad .$$

The inner integration is by definition the Complementary Error function,

$$\text{Erfc}(\frac{x}{2\sqrt{m^2\tau - x}}), \quad \text{Thus}$$

$$T = \frac{1}{\Gamma(\omega)}(\frac{m^2R^2}{4})^{\omega}\int_0^{m^2\tau} \exp\{\frac{-m^2R^2}{4x}\} \text{Erfc}\{\frac{x}{2\sqrt{m^2\tau - x}}\} \frac{dx}{x^{1+\omega}}$$

Making the change of variable, $y = \frac{m^2R^2}{4x}$, in the above equation results in

$$T = \frac{1}{\Gamma(\omega)} \int_u^\infty \exp\{-y\}\mathrm{Erfc}\left(\frac{m^2R^2}{8y}\left(m^2\tau - \frac{m^2R^2}{4y}\right)^{-1/2}\right) y^{\omega-1} dy \quad .$$

Rearranging the argument of the Complementary Error function in the integrand results in

$$\frac{m^2R^2}{8y}\left(m^2\tau - \frac{m^2R^2}{4y}\right)^{-1/2} = \eta \frac{\sqrt{u}}{\sqrt{y(y-u)}} \quad ,$$

where

$$\eta = \frac{KR}{4\alpha} = \frac{1}{2} \frac{r}{b_m} \left[\frac{K_r}{K_m} \frac{(\rho C)_r}{(\rho C)_m}\right]^{1/2} \quad .$$

Consequently,

$$T = \frac{1}{\Gamma(\omega)} \int_0^\infty \exp(-y)\ \mathrm{Erfc}\left(\eta \frac{\sqrt{u}}{\sqrt{y(y-u)}}\right) y^{\omega-1}\ dy \quad . \quad \ldots\ldots\ [C-21]$$

APPENDIX D

COMPUTER PROGRAMS USED IN THIS STUDY

Four computer programs are listed in this appendix. They are: (1) Main Program for Short Time Period Solution, (2) Main Program for Long Time Period Solution, (3) Main Program for Steady State Solution, and (4) Subroutines Commonly Used for Three Solutions.

All real variables used in these four programs are double-precisioned and have their definitions stated at the beginning of each of the main program(Programs 1, 2 and 3). The fourth program (Subroutines Commonly Used for Three Solutions) contains two subroutines, 32-Point Ganssian Quadrature and Gamma Function in Logarithm, which are called in each of the main program (Programs 1, 2 and 3).

```
C*************************************************************************
C                    M A I N   P R O G R A M                             *
C     F O R   S H O R T   T I M E   P E R I O D   S O L U T I O N        *
C                                                                        *
C     THIS PROGRAM READS IN THE THERMAL AND PHYSICAL DATA OF THE         *
C     PROBLEM , AND DETERMINS THE DIMENSIONLESS AQUIFER TEMPERATURE.     *
C     ALL THE REAL VARIABLES IN THIS PROGRAM ARE DOUBLE-PRECISIONED.     *
C                                                                        *
C     BM = AQUIFER THICKNESS                                             *
C     BR = CAPROCK THICKNESS                                             *
C     XKM = AQUIFER THERMAL CONDUCTIVITY                                 *
C     XKR = CAPROCK THERMAL CONDUCTIVITY                                 *
C     ROCM = AQUIFER THERMAL CAPACITYITY                                 *
C     ROCR = CAPROCK THERMAL CAPACITYITY                                 *
C     ROCF = INJECTED FLUID THERMAL CAPACITY                             *
C     Q = INJECTION RATE
C                                                                        *
C*************************************************************************
C                                                                        *
      IMPLICIT REAL*8(A-H,O-Z)
      COMMON W,DW,U,ETA
C                                                                        *
C                       D A T A   I N P U T                              *
C                                                                        *
      READ,BM
      READ,BR
      READ,XKM
      READ,XKR
      READ,ROCM
      READ,ROCR
      READ,ROCF
      READ,Q
C                                                                        *
C           P A R A M E T E R   D E T E R M I N A T I O N                *
C                                                                        *
```

```
      BB=2.0D0*BR/BM
      W=ROCF*Q/4.0D0/3.14159/BM/XKM
      CALL DLGAM(W,DW,IER)
      ALFM=XKM/ROCM
      ALFR=XKR/ROCR
      ALF=DSQRT(ALFR/ALFM)
      XK=XKR/XKM
      ETA1=XK/ALF/4.0D0
      TAU1=4.0D0*ALFM/BM/BM
      PRINT 10,W,ALFM,ALFR,ALF,XK,BB
10    FORMAT(/,10X,'W=',D13.6,5X,'ALFM=',D13.6,5X,'ALFR=',D13.6,5X,'ALF=
     C',D13.6,5X,'K=',D13.6,5X,'B=',D13.6)
C                                                                      *
C                        T I M E   I N P U T                           *
C                                                                      *
1     READ,TIME
      IF(TIME.LT.0.0D0) STOP
      TAU=TIME*TAU1
      PRINT 12,TIME,TAU
12    FORMAT(/,10X,'TIME=',D13.6,5X,'TAU=',D13.6)
C                                                                      *
C     R A D I A L   D I S T A N C E   D E T E R M I N A T I O N        *
C                                                                      *
      R=0.0D0
2     IF(R.LT.100000.0D0) DR=5000.0D0
      IF(R.LT.10000.0D0) DR=500.0D0
      IF(R.LT.1000.0D0) DR=50.0D0
      IF(R.LT.100.0D0) DR=10.0D0
      R=R+DR
      RO=2.0D0*R/BM
C                                                                      *
C                A Q U I F E R   T E M P E R A T U R E                 *
C                      D E T E R M I N A T I O N                       *
C                                                                      *
      ETA=RO*ETA1
      U=RO*RO/TAU/4.0D0
```

```
      CALL SHORT(SOL)
      PRINT 20, R,SOL
20    FORMAT(10X,'R= ',D13.6,10X,'TEMP.= ',D13.6)
      IF(SOL.GT.0.01) GO TO 2
      GO TO 1
      END
C
C
C*****************************************************************************
C              S U B R O U T I N E   S H O R T                              *
C                                                                           *
C     IN THIS SUBROUTINE , THE 32-POINT GAUSSIAN QUADRATURE IS USED TO      *
C     NUMERICALLY INTEGRATE THE SOLUTION , AN EXTERNAL FUNCTION , FCT1      *
C     , IS USED TO CALCULATE THE INTEGRAND OF THE INTEGRAL.                 *
C                                                                           *
C*****************************************************************************
      SUBROUTINE SHORT(YY)
      IMPLICIT REAL*8(A-H,O-Z)
      EXTERNAL FCT1
      COMMON W,DW,U,ETA
      XL=U
      XU=2.50D0*W
      IF(XL.GT.XU) GO TO 1
      CALL DQG32(XL,XU,FCT1,Y)
      YY=Y
      RETURN
1     YY=0.0D0
      RETURN
      END
C
C                                                                           *
C                  E X T E R N A L   F U N C T I O N                        *
C                                                                           *
      FUNCTION FCT1(X)
      IMPLICIT REAL*8(A-H,O-Z)
      COMMON W,DW,U,ETA
```

```
      ERX=ETA*DSQRT(U/X/(X-U))
      IF(ERX.GT.13.30D0) GO TO 1
      A=DERFC(ERX)
      PD=-X+(W-1.0D0)*DLOG(X)+DLOG(A)-DW
      IF(PD.LT.-50.0D0) GO TO 1
      FCT1=DEXP(PD)
      RETURN
1     FCT1=0.0
      RETURN
      END
C
C
```

```
C*************************************************************************
C                    M A I N   P R O G R A M                            *
C      F O R   L O N G   T I M E   P E R I O D   S O L U T I O N        *
C                                                                       *
C      THIS PROGRAM READS IN THE THERMAL AND PHYSICAL DATA OF THE       *
C      PROBLEM . AND DETERMINS THE DIMENSIONLESS AQUIFER TEMPERATURE.   *
C      ALL THE REAL VARIABLES IN THIS PROGRAM ARE DOUBLE-PRECISIONED.   *
C                                                                       *
C      BM = AQUIFER THICKNESS                                           *
C      BR = CAPROCK THICKNESS                                           *
C      XKM = AQUIFER THERMAL CONDUCTIVITY                               *
C      XKR = CAPROCK THERMAL CONDUCTIVITY                               *
C      ROCM = AQUIFER THERMAL CAPACITYITY                               *
C      ROCR = CAPROCK THERMAL CAPACITYITY                               *
C      ROCF = INJECTED FLUID THERMAL CAPACITY                           *
C      Q = INJECTION RATE                                               *
C                                                                       *
C*************************************************************************
C                                                                       *
      IMPLICIT REAL*8(A-H,O-Z)
      COMMON W,DW,U,SIGMA
C                                                                       *
C                        D A T A   I N P U T                            *
C                                                                       *
      READ,BM
      READ,BR
      READ,XKM
      READ,XKR
      READ,ROCM
      READ,ROCR
      READ,ROCF
      READ,Q
C                                                                       *
C            P A R A M E T E R   D E T E R M I N A T I O N              *
C                                                                       *
```

```
      BB=2.0D0*BR/BM
      W=ROCF*Q/4.0D0/3.14159/BM/XKM
      CALL DLGAM(W,DW,IER)
      ALFM=XKM/ROCM
      ALFR=XKR/ROCR
      ALF=DSQRT(ALFR/ALFM)
      XK=XKR/XKM
      SIGMA1=XK/BB/4.0D0
      TAU1=4.0D0*ALFM/BM/BM
      DELTA=XK*BB/ALF/ALF/3.0D0
      PRINT 10, W,ALFM,ALFR,ALF,XK,BB,DELTA
10    FORMAT(/,10X,'W=',D13.6,5X,'ALFM=',D13.6,5X,'ALFR=',D13.6,5X,'ALF=
     C',D13.6,5X,'K=',D13.6,5X,'B=',D13.6,/,10X,'DELTA= ',D13.6)
C                                                                       *
C                        T I M E   I N P U T                            *
C                                                                       *
1     READ,TIME
      IF(TIME.LT.0.0D0) STOP
      TAU=TIME*TAU1
      PRINT 12,TIME,TAU
12    FORMAT(/,10X,'TIME=',D13.6,5X,'TAU=',D13.6)
C                                                                       *
C     R A D I A L   D I S T A N C E   D E T E R M I N A T I O N         *
C                                                                       *
      R=0.0D0
2     IF(R.LT.100000.0D0) DR=5000.0D0
      IF(R.LT.10000.0D0) DR=500.0D0
      IF(R.LT.1000.0D0) DR=50.0D0
      IF(R.LT.100.0D0) DR=10.0D0
      R=R+DR
      RO=2.0D0*R/BM
C                                                                       *
C                A Q U I F E R   T E M P E R A T U R E                  *
C                      D E T E R M I N A T I O N                        *
C                                                                       *
      U=RO*RO/TAU/4.0D0
```

```
      U=(1.0D0+DELTA)*U
      SIGMA=RO*RO*SIGMA1
      CALL XLONG(SOL)
      PRINT 20, R,SOL
20    FORMAT(10X,'R= ',D13.6,10X,'TEMP.= ',D13.6)
      IF(SOL.GT.0.01) GO TO 2
      GO TO 1
      END
C
C
C*********************************************************************
C              S U B R O U T I N E   X L O N G                      *
C                                                                   *
C     IN THIS SUBROUTINE , THE 32-POINT GAUSSIAN QUADRATURE IS USED TO *
C     NUMERICALLY INTEGRATE THE SOLUTION , AN EXTERNAL FUNCTION , FCT3 *
C     , IS USED TO CALCULATE THE INTEGRAND OF THE INTEGRAL.         *
C                                                                   *
C*********************************************************************
      SUBROUTINE XLONG(YY)
      IMPLICIT REAL*8(A-H,O-Z)
      EXTERNAL FCT3
      COMMON W,DW,U,SIGMA
      XL=U
      XU=2.50D0*W
      IF(XL.GT.XU) GO TO 1
      CALL DQG32(XL,XU,FCT3,Y)
      YY=Y
      RETURN
1     YY=0.0D0
      RETURN
      END
C
C                                                                   *
C                 E X T E R N A L   F U N C T I O N                 *
C                                                                   *
      FUNCTION FCT3(X)
```

```
      IMPLICIT REAL*8(A-H,O-Z)
      COMMON W,DW,U,SIGMA
      PO=-X-(SIGMA/X)+(W-1.0D0)*DLOG(X)-DW
      IF(PO.LT.-50.0D0) GO TO 1
      FCT3=DEXP(PO)
      RETURN
1     FCT3=0.0D0
      RETURN
      END
C
C
```

```
C*****************************************************************
C                    M A I N   P R O G R A M                     *
C            F O R   S T E A D Y   S T A T E   S O L U T I O N   *
C                                                                *
C      THIS PROGRAM READS IN THE THERMAL AND PHYSICAL DATA OF THE *
C      PROBLEM , AND DETERMINS THE DIMENSIONLESS AQUIFER TEMPERATURE.*
C      ALL THE REAL VARIABLES IN THIS PROGRAM ARE DOUBLE-PRECISIONED.*
C                                                                *
C      BM = AQUIFER THICKNESS                                    *
C      BR = CAPROCK THICKNESS                                    *
C      XKM = AQUIFER THERMAL CONDUCTIVITY                        *
C      XKR = CAPROCK THERMAL CONDUCTIVITY                        *
C      ROCM = AQUIFER THERMAL CAPACITYITY                        *
C      ROCR = CAPROCK THERMAL CAPACITYITY                        *
C      ROCF = INJECTED FLUID THERMAL CAPACITY                    *
C      Q = INJECTION RATE
C                                                                *
C*****************************************************************
C                                                                *
      IMPLICIT REAL*8(A-H,O-Z)
      COMMON W,DW,SIGMA
C                                                                *
C                       D A T A   I N P U T                      *
C                                                                *
      READ,BM
      READ,BR
      READ,XKM
      READ,XKR
      READ,ROCM
      READ,ROCR
      READ,ROCF
      READ,Q
C                                                                *
C           P A R A M E T E R   D E T E R M I N A T I O N        *
C                                                                *
```

```
      BB=8.0D0*R/BM
      W=ROCP*Q/4.0D0/3.14159/BM/XKM
      CALL DLGAM(W,DW,IER)
      ALFM=XKM/ROCM
      ALFR=XKR/ROCR
      ALF=DSQRT(ALFR/ALFM)
      XK=XKR/XKM
      SIGMA1=XK/BB/4.0D0
      PRINT 10,W,ALFM,ALFR,ALF,XK,BB
10    FORMAT(/,10X,'W=',D13.6,5X,'ALFM=',D13.6,5X,'ALFR=',D13.6,5X,'ALF=
     C',D13.6,5X,'K=',D13.6,5X,'B=',D13.6)
C                                                                       *
C     R A D I A L   D I S T A N C E   D E T E R M I N A T I O N         *
C                                                                       *
      R=0.0D0
2     IF(R.LT.100000.0D0) DR=5000.0D0
      IF(R.LT.10000.0D0) DR=500.0D0
      IF(R.LT.1000.0D0) DR=50.0D0
      IF(R.LT.100.0D0) DR=10.0D0
      R=R+DR
      RO=2.0D0*R/BM
C                                                                       *
C                A Q U I F E R   T E M P E R A T U R E                  *
C                      D E T E R M I N A T I O N                        *
C                                                                       *
      SIGMA=RO*RO*SIGMA1
      CALL STDBK(SOL)
      PRINT 20, R,SOL
20    FORMAT(10X,'R= ',D13.6,10X,'TEMP.= ',D13.6)
      IF(SOL.LT.0.01) GO TO 2
      STOP
      END
C
C
C***********************************************************************
C              S U B R O U T I N E   S T D B K                          *
```

```
C                                                                       *
C     IN THIS SUBROUTINE , THE 32-POINT GAUSSIAN QUADRATURE IS USED TO  *
C     NUMERICALLY INTEGRATE THE SOLUTION . AN EXTERNAL FUNCTION , FCT2  *
C     , IS USED TO CALCULATE THE INTEGRAND OF THE INTEGRAL.             *
C                                                                       *
C***********************************************************************
      SUBROUTINE STCBK(YY)
      IMPLICIT REAL*8(A-H,O-Z)
      EXTERNAL FCT2
      COMMON W,DW,SIGMA
      YY=0.0D0
      XMAX=1.0D0/((1.0D0+W)+(SIGMA/(1.0D0+W)))
      XL=0.50D0*XMAX
      XU=XMAX
      CALL DQG32(XL,XU,FCT2,Y)
      YY=YY+Y
      XL=XU
      XU=2.5D0*XMAX
      CALL DQG32(XL,XU,FCT2,Y)
      YY=YY+Y
      YY=1.0D0-YY
      RETURN
      END
C
C                                                                       *
C                  E X T E R N A L    F U N C T I O N                 *
C                                                                       *
      FUNCTION FCT2(X)
      IMPLICIT REAL*8(A-H,O-Z)
      COMMON W,DW,SIGMA
      EEP=-SIGMA*X
      IF(EEP.LT.-170.0D0) EEP=-170.0D0
      EP=1.0D0-DEXP(EEP)
      PPO=-1.0D0/X+DLOG(EP)-(1.0D0+W)*DLOG(X)-DW
      IF(PPO.LT.-50.0D0) GO TO 1
      FCT2=DEXP(PPO)
```

```
      RETURN
1     FCT2=0.000
      RETURN
      END
C
C
```

```
C*******************************************************************
C                                                                  *
C          S U B R O U T I N E S    C O M M O N L Y    U S E D     *
C               F O R    T H R E E    S O L U T I O N S           *
C                                                                  *
C*******************************************************************
C
C
C*******************************************************************
C                                                                  *
C                     32-POINT  GAUSSIAN  QUADRATURE               *
C                                                                  *
C*******************************************************************
      SUBROUTINE DQG32(XL,XU,FCT,Y)
      IMPLICIT REAL*8(A-H,O-Z)
      A=.5D0*(XU+XL)
      B=XU-XL
      C=.4986319309247408D0*B
      Y=.3509305004735048D-2*(FCT(A+C)+FCT(A-C))
      C=.4928057557726342D0*B
      Y=Y+.8137197365452835D-2*(FCT(A+C)+FCT(A-C))
      C=.4823811277937532D0*B
      Y=Y+.1269603265463103D-1*(FCT(A+C)+FCT(A-C))
      C=.4674530379688698D0*B
      Y=Y+.1713693145651072D-1*(FCT(A+C)+FCT(A-C))
      C=.4481605778830261D0*B
      Y=Y+.2141794901111334D-1*(FCT(A+C)+FCT(A-C))
      C=.4246838068662850D0*B
      Y=Y+.2549029631188809D-1*(FCT(A+C)+FCT(A-C))
      C=.3972418979839712D0*B
      Y=Y+.2934204673926777D-1*(FCT(A+C)+FCT(A-C))
      C=.3660910593701448D0*B
      Y=Y+.3291111138818092D-1*(FCT(A+C)+FCT(A-C))
      C=.3315221234651076D0*B
      Y=Y+.3611[illegible]*(FCT(A+C)+FCT(A-C))
```

```
      C=.[illegible]
      Y=Y+.[illegible](A+C)+FCT(A-C))
      C=.25344995446611470D0*B
      Y=Y+.41655962113473380-1*(FCT(A+C)+FCT(A-C))
      C=.21067563806531770D0*B
      Y=Y+.43826046502201910-1*(FCT(A+C)+FCT(A-C))
      C=.16593430114106380D0*B
      Y=Y+.45586939347881940-1*(FCT(A+C)+FCT(A-C))
      C=.11964368112606850D0*B
      Y=Y+.46922199540402280-1*(FCT(A+C)+FCT(A-C))
      C=.72235980791398250-1*B
      Y=Y+.47819360039637430-1*(FCT(A+C)+FCT(A-C))
      C=.24153832843869160-1*B
      Y=B*(Y+.48270044257363900-1*(FCT(A+C)+FCT(A-C)))
      RETURN
      END
C
C
C*************************************************************************
C                                                                        *
C                    GAMMA  FUNCTION  IN  LOGRITHM                       *
C                                                                        *
C*************************************************************************
       SUBROUTINE DLGAM(XX,DLNG,IER)
      DOUBLE PRECISION XX,ZZ,TERM,DLNG,RZ2
      IER=0
      ZZ=XX
      IF(XX-1.D10) 2,2,1
1     IF(XX-1.D70) 8,9,9
  2   IF(XX-1.D-9) 3,3,4
3     IER=-1
      DLNG=-1.D75
      GO TO 10
4     TERM=1.D0
5     IF([illegible]) 6,6,7
6     [illegible]22
```

```
      [illegible]
      [illegible]
7     RZ2=1.D0/ZZ**2
      DLNG=(ZZ-0.5D0)*DLOG(ZZ)-ZZ+.9189385332046727-DLOG(TERM)+
     1(1.D0/ZZ)*(.83333333333333333D-1-(RZ2*(.27777777777777777D-2+(RZ2*
     2(.79365079365079365D-3-(RZ2*(.59523809523809523D-3))))))))
      GO TO 10
8     DLNG=ZZ*(DLOG(ZZ)-1.D0)
      GO TO 10
9     IER=+1
      DLNG=1.D75
10    RETURN
      END
C
```